Plant Direct

WILEY

American Society of Plant Biologists SEB SOCIETY FOR EXPERIMENTAL BIOLOGY

RESEARCH ARTICLE OPEN ACCESS

Unequal Genetic Redundancies Among MYC bHLH Transcription Factors Underlie Seedling Photomorphogenesis in Arabidopsis

Vikas Garhwal | Sreya Das | Sreeramaiah N. Gangappa

Department of Biological Sciences, Indian Institute of Science Education and Research Kolkata, Mohanpur, India

Correspondence: Sreeramaiah N. Gangappa (ngsreeram@iiserkol.ac.in)

Received: 5 July 2024 | **Revised:** 18 December 2024 | **Accepted:** 9 January 2025

Funding: This work was supported by grants from the Department of Biotechnology (Ramalingaswami Re-entry Fellowship grant, BT/RLF/Re-entry/28/2017), Science and Engineering Research Board (start-up research grant, SRG/2019/000446) from the Govt. of India, and Intramural grant from IISER Kolkata (Ministry of Education, Govt. of India) to S.N.G.

Keywords: COP1 | HY5 | MYC2 | MYC3 | MYC4 | photomorphogenesis | ubiquitination

ABSTRACT

Light is one of the most critical ecological cues controlling plant growth and development. Plants have evolved complex mechanisms to cope with fluctuating light signals. In Arabidopsis, bHLH transcription factors MYC2, MYC3, and MYC4 have been shown to play a vital role in protecting plants against herbivory and necrotrophic pathogens. While the role of MYC2 in light-mediated seedling development has been studied in some detail, the role of MYC3 and MYC4 still needs to be discovered. Here, we show that MYC4 negatively regulates seedling photomorphogenesis, while the MYC3 function seems redundant. However, the genetic analysis reveals that MYC3/MYC4 together act as positive regulators of seedling photomorphogenic growth as the *myc3myc4* double mutants showed exaggerated hypocotyl growth compared to the *myc3* and *myc4* single mutants and Col-0. Intriguingly, the loss of *MYC2* function in the *myc3myc4* double mutant background (*myc2myc3myc4*) resulted in further enhancement in the hypocotyl growth than *myc3myc4* double mutants in WL, BL and FRL, suggesting that MYC2/3/4 together play an essential and positive role in meditating optimal seedling photomorphogenesis. Besides, MYC3/MYC4 genetically and physically interact with HY5 to partially inhibit its function in controlling hypocotyl and photo-pigment accumulation. Moreover, our results suggest that COP1 physically interacts and degrades MYC3 and MYC4 through the 26S proteasomal pathway and controls their response to dark and light for fine-tuning HY5 function and seedling photomorphogenesis.

1 | Introduction

Light is a potent stimulus that regulates plant development and phenotypic plasticity. Plant development, including seed germination, photomorphogenesis, leaf development, petiole elongation, shade avoidance, and flowering, is dependent on the presence or absence of light (Cheng et al. 2021; Krahmer and Fankhauser 2023; Huq, Lin, and Quail 2024). Light drives transition in the development of plants: Photomorphogenesis or de-etiolation happens as soon as a seedling emerges from the soil and sees the light for the first time. There are two contrasting patterns in the seedlings stage: Skotomorphogenesis and photomorphogenesis. Several physiological responses change with the transition from skotomorphogenic to photomorphogenic seedling development, like opening of apical hook, expansion of cotyledons, inhibition of hypocotyl elongation, far-red light-controlled blocking of greening, and accumulation of chlorophyll and anthocyanin (Nagatani, Reed, and Chory 1993; Whitelam et al. 1993; Neff, Fankhauser, and Chory 2000). Many downstream components in light signal transduction have

been reported and characterized as involved in photomorphogenic growth and development (Jiao, Lau, and Deng 2007; Lee et al. 2007). A group of negative regulators known as COP/DET/FUS works downstream of numerous photoreceptors to suppress photomorphogenic development and light-induced gene expression (Wei and Deng 1999; Jiao, Lau, and Deng 2007; Lau and Deng 2012). CONSTITUTIVE PHOTOMORPHOGENIC 1 (COP1) acts as a ubiquitin ligase and degrades the photomorphogenesis-promoting factors such as ELONGATED HYPOCOTYL5 (HY5), HY5 HOMOLOG (HYH), LONG AFTER FAR-RED LIGHT 1 (LAF1), LONG HYPOCOTYL IN FARRED 1 (HFR1) and B-box (BBX)-containing protein BBX21 (also known as SALT TOLERANCE HOMOLOG 2), and so on, in the dark (Osterlund, Wei, and Deng 2000; Holm et al. 2002; Seo et al. 2003; Jang et al. 2005; Yang et al. 2005; Xu et al. 2016; Blanco-Touriñán et al. 2020). Reports have shown that COP1 interacts with SUPPRESSOR OF PHYA-105 1 (SPA1), which facilitates the modulation of the proteasome-mediated degradation of HY5, HFR1, and LAFl (Saijo et al. 2003; Seo et al. 2003). The control of HY5 by COP1 is one of the primary mechanisms by which a plant decides between skotomorphogenesis and photomorphogenesis (Ang and Deng 1994; Ang et al. 1998; Osterlund, Wei, and Deng 2000; Holm et al. 2002; Lau and Deng 2012).

HY5, a basic domain/leucine zipper (bZIP) transcription factor, is critical for light-mediated seeding photomorphogenic growth (Oyama, Shimura, and Okada 1997; Chattopadhyay et al. 1998; Gangappa and Botto 2016; Burko et al. 2020). The *hy5* mutant seedlings have a partially etiolated hypocotyl phenotype with reduced chlorophyll and anthocyanin accumulation in white light and different wavelengths of light, such as red, far-red, and blue light, in addition to having more lateral roots compared with wild-type plants (Koornneef, Rolff, and Spruit 1980; Oyama, Shimura, and Okada 1997; Chattopadhyay et al. 1998). Moreover, HY5 also functions in UV-B light as a positive regulator of UV-B signaling (Binkert et al. 2014a). HY5 functions cooperatively and antagonistically with various other transcription factors such as HYH, HFR1, CALMODULIN 7(CAM7), Z-box binding factors (ZBFs) MYC2, G-BOX BINDING FACTOR 1 (GBF1), TANDEM ZINC-FINGER/PLUS3 (TZP), and many of the BBX class of proteins either by acting as transcriptional co-activators or co-repressors (Holm et al. 2002; Datta et al. 2008; Gangappa et al. 2013a; Ram and Chattopadhyay 2013; Abbas et al. 2014; Binkert et al. 2014b; Gangappa and Botto 2016; Chakraborty et al. 2019; Song et al. 2020; Job and Datta 2021; Li et al. 2022). In Arabidopsis, bHLH transcription factors, such as MYC2, MYC3, and MYC4, have been shown to play a vital role in inducing defense responses against herbivory (Dombrecht et al. 2007; Chico et al. 2014; Zhang et al. 2014; Wang et al. 2021). MYC2, MYC3, and MYC4 are basic helix–loop–helix transcription factors that interact with Jasmonate Zim-domain proteins and are their direct targets. These transcription factors (TFs) have been demonstrated to work together to govern Arabidopsis growth and development (Gao et al. 2016). MYC3 is a JAZ-interacting transcription factor that acts with MYC2 and MYC4 to activate JA responses (Fernandez-Calvo et al. 2011). Recent studies have also highlighted the importance of MYC2 and MYC4 transcription factors in the regulation of secondary cell wall thickening in response to blue light (BL) and red light (RL) by regulating the expression of genes involved in the secondary cell wall thickening (Zhang et al. 2018; Luo et al. 2022).

Unequal genetic redundancy is a common phenomenon observed in Arabidopsis and is likely in crops and other plants (Laubinger, Fittinghoff, and Hoecker 2004; Dohmann, Kuhnle, and Schwechheimer 2005; Briggs et al. 2006; Sibout et al. 2006). For example, MYC2 shows unequal genetic redundancy with a bZIP transcription factor G-BOX BINDING FACTOR1 (GBF1) in regulating hypocotyl growth (Maurya et al. 2015). Both *myc2* and *gbf1* have shorter hypocotyl than the wild-type (Yadav et al. 2005; Mallappa et al. 2006); in the *myc2gbf1* double mutant, instead of enhancing the short hypocotyl phenotype, they suppressed their short hypocotyl phenotype and had hypocotyl length similar to the wild-type (Maurya et al. 2015). Similarly, *spa1* mutants have a reduced hypocotyl length, while *spa2* mutants show a hypocotyl length similar to that of wild-type. However, the *spa1spa2* double mutants show shorter hypocotyls than the *spa1*, suggesting that SPA1 and SPA2 show unequal redundancy in controlling hypocotyl growth (Laubinger, Fittinghoff, and Hoecker 2004). Similarly, the two closely related bZIP transcription factors, which are key regulators of photomorphogenic growth, showed reduced root system growth phenotype in the *hy5hyh* double mutants than in the single mutants, wherein the root system growth is enhanced (Sibout et al. 2006). The COP9 signalosome (CSN) components, CSN5A and CSN5B, also have similar genetic interactions for the regulation of seedling photomorphogenesis and lateral root development, as the *csn5b* mutant does not show any phenotypic changes further enhance the *csn5a* mutant phenotypes (Dohmann, Kuhnle, and Schwechheimer 2005).

Among MYCs, the role of MYC2 in Arabidopsis seedling development is very well established. MYC2 is a key regulator of seedling photomorphogenesis and light-induced gene expression (Yadav et al. 2005; Gangappa, Prasad, and Chattopadhyay 2010; Sethi et al. 2014; Maurya et al. 2015; Chakraborty et al. 2019; Srivastava et al. 2022; Ojha et al. 2023). While the role of MYC2 in light-mediated seedling development has been studied to some extent, that of MYC3 and MYC4 remains unknown. Here, we focus on understanding the genetic and molecular interactions of MYC3 and MYC4 in seedling development. We found that MYC3 and MYC4 show unequal genetic redundancies with MYC2. While MYC4 is a negative regulator of light-mediated inhibition of hypocotyl growth, together with MYC3 and MYC2, act to promote seedling photomorphogenesis. Further, we report the genetic and biochemical interaction studies between COP1 and HY5 in regulating seedling photomorphogenesis. Our study revealed that the stability of MYC3 and MYC4 is controlled by COP1 under both light and dark conditions, likely through ubiquitination and degradation. Our findings unravel the hitherto unknown interactions among MYC transcription factors in regulating seedling photomorphogenesis.

2 | Materials and Methods

2.1 | Plant Materials and Growth Condition

All genotypes used in this study are in *Arabidopsis thaliana* Columbia ecotype (Col-0) background, which was used as wild-type. The *myc2-2* (SALK_040500), *myc3-1* (GK_445B11), *myc3-2* (SALK_012763), *myc4-1* (GK_491E10), and *myc4-2* (SALK_052158) have been ordered from the Nottingham

Arabidopsis Stock Centre (NASC). The *myc2* (*jin1-2*) allele (Lorenzo et al. 2004), *cop1-4* (McNellis et al. 1994) and *hy5-215* (Oyama, Shimura, and Okada 1997) are described elsewhere. The *35S:MYC3-GFP* and *35S:MYC4-GFP* are described elsewhere (Fernandez-Calvo et al. 2011). All the mutants used in this study are in Col-0 background.

The seeds were surface sterilized (70% ethanol + 0.05% Triton X-100) and plated on Murashige and Skoog agar medium (MS plates) with 1% sucrose and 0.8% agar (HiMedia, RM7691). The plates were then kept in the dark for stratification for 4 days at 4°C and transferred to light chambers maintained at 22°C with the required wavelength and intensity. The 100–120 $\mu mol\, m^{-2}\, s^{-1}$ light intensity is used to grow seedlings for all the experiments under WL. Experiments were performed under specified short-day conditions (8-h-light/16-h-dark) or long-day (16-h-light/8-h-dark) conditions. For monochromatic light, different wavelengths of light (60 $\mu mol\, m^{-2}\, s^{-1}$ for RL, 35 $\mu mol\, m^{-2}\, s^{-1}$ for BL, and 0.5 $\mu mol\, m^{-2}\, s^{-1}$ for FRL) were used.

2.2 | Generation of Double and Triple Mutants

For the generation of the *myc3myc4* (*myc34*) double-mutant, homozygous *myc3* mutant plants were crossed with *myc4* homozygous lines. The F_2 seedlings were selected in MS with sulfadiazine antibiotic plates. The F_2 plants were then tested by genomic PCR for both *myc3* and *myc4* loci. The F_3 progeny that is homozygous for *myc3* and *myc4* mutation is further tested by genotypic PCR and is designated as *myc34* double mutant. The *myc2myc3myc4* triple mutants were generated by crossing the *myc34* double mutant with the *myc2* (*jin1-2*) allele.

In the same process, single mutant *myc3* and *myc4* were crossed with the *hy5* homozygous mutant, respectively. The *hy5* mutant seedlings were selected in the F_2 population. F2 plants were then individually tested by genomic PCR for the myc3 and myc4 locus. F3 progeny that is homozygous for *myc3* mutation was further tested by genotypic PCR and designated as *myc3hy5* double-mutants, and those that are homozygous for *myc4* mutation and PCR tested were designated as *myc4hy5* double-mutants. The homozygous *myc3myc4* double mutants were crossed with the *hy5* mutant to generate a triple mutant of *myc3myc4hy5* (*myc34hy5*). In the same way, *myc3cop1-4, myc4cop1-4*, and *myc34cop1-4* mutants were generated through genetic crossing. In all the cases, homozygous seeds were confirmed by PCR screening and bulked seeds for the experiments.

Transgenic seedlings overexpressing MYC3 and MYC4 in *cop1-4* mutants were generated by genetic crosses using *cop1-4* single mutants as females and MYC3 and MYC4 transgenic lines as males in each of the individual crosses. Seedlings with *cop1* mutant phenotype were selected in F_2 populations, and the overexpression of *MYC3-OE* and *MYC4-OE* transgene in *cop1-4* mutant was confirmed by antibiotic resistance and western blot (using anti-GFP antibodies). Several homozygous lines were reconfirmed in F3 generation and were used for further studies.

2.3 | Easy Plant DNA Extraction for Genotyping the Mutants

Small leaf discs were collected in 40 µL of 0.25 M NaOH in sterile Eppendorfs. Samples were incubated in a dry-bath for 30 s. Samples are neutralized by adding 40 µL of 0.25 M HCl and 20 µL of 0.5 M Tris–HCl of pH 8.0 containing 0.25% (V/V) NP-40 or triton-X 100. The samples were boiled again for 2 mins and stored at 4°C before proceeding with PCR.

2.4 | Hypocotyl Length Measurement

Six-day-old seedlings grown as specified above are used for hypocotyl measurements. At least 20–25 seedlings were aligned on a 1% agar plate containing 1% charcoal and imaged using a digital camera, and hypocotyl lengths were measured using NIH ImageJ software.

2.5 | Genomic DNA Extraction

Rapid genomic DNA extraction was performed using cetyltrimethylammonium bromide (CTAB). The young rosette leaf/tissue was harvested in liquid nitrogen and ground the tissue in a 1.5-mL microcentrifuge tube, and 500 µL of fresh CTAB DNA extraction buffer (1.4 M NaCl, 20 mM EDTA, 100 mM Tris–HCl pH = 8.0, 2% CTAB powder, 0.2% β-ME) was added. The solution was mixed and vortexed thoroughly. The samples were kept on ice until all the samples were ready for the next step. Next, the homogenate was transferred to a 60°C water bath for 30 min. The homogenate was centrifuged at 13000 rpm for 10 min. The supernatant was transferred to a new tube, and 2 µL of 10 mg/mL RNase Solution A was added and incubated at 37°C for another 30 min. An equal volume of phenol:chloroform: isoamyl alcohol (25:24:1, Sigma) was added and mixed by gently inverting the tube to avoid shearing the DNA. The solution was then centrifuged at 130000 rpm for 10 min to separate the phase. Next, the aqueous upper phase was transferred to a new microcentrifuge tube, and this step was repeated until the upper phase was clear. The DNA was precipitated by adding 0.7 volume of cold isopropanol, and the tube was inverted gently to mix and incubate at −20°C for 60 min. Then, the sample was centrifuged at 13000 rpm for 20 min. The supernatant was decanted without disturbing the pellet. The pellet was washed with 500 µL of ice-cold 70% ethanol (Merck) and centrifuged at 13000 rpm for 5 min. The pellet was air-dried until the smell of ethanol went away. Finally, the pellet was dissolved with 100 µL TE buffer (10 mM Tris–HCL, pH = 8.0, 1 mM EDTA), and genotyping PCR was done using a dCAPs marker. The PCR product was digested with *ApaL1* restriction enzyme overnight and run in 2.5% agarose gel.

2.6 | RNA Extraction and Gene Expression Analysis by qPCR

Six-day-old dark/light-grown seedlings were used for total RNA isolation. Approximately 100 mg of plant seedlings/other tissues were powdered using liquid nitrogen before extracting total RNA using RNeasy® Plant Mini Kit (QIAGEN) with on-column DNase I digestion according to the manufacturer's instructions. The

integrity of RNA was quantified by Nanodrop. Approximately 2.0 μg of total RNA was converted into cDNA using a verso cDNA synthesis kit (Thermo-Fisher scientific; AB-1453/B) and oligo dT following the manufacturer's instructions. The 2.0 μL of 1:20 diluted cDNA was used for qPCR using PowerUp SYBR Green Master Mix. qPCR experiments were performed in QuantStudio™ 5 Real-Time PCR System. *EF1α* (AT5G60390) was used as an internal control for normalization. Details of the oligonucleotide primers used are provided in Table S1.

2.7 | Anthocyanin Level Measurement for Arabidopsis Seedlings

The anthocyanin level was measured by following the protocol described before (Holm et al. 2002). About 20–30 seedlings are taken into a microcentrifuge tube and weighed (around 35–50 mg); 400 μL of extraction solution (1% HCL in Methanol) is added and vortexed very well and kept at 4°dark conditions overnight. The next day, the seedlings were crushed, and 200 μL of sterile water and 200 μL of chloroform were added. The debris was removed by centrifugation (10 min, 13,000 rpm), and the supernatant was collected into a fresh microcentrifuge tube. Then, spectrophotometric estimation is carried out by taking readings at 530 and 657 nm wavelengths. The total Anthocyanin content is calculated with the help of the following formula: $(A_{530}-0.33A_{657})$/gm of tissue.

2.8 | Chlorophyll Estimation for Arabidopsis Seedlings

The chlorophyll level was measured by following the protocol described by Holm et al. 2002. Approximately 30–40 6-day-old seedlings were collected, weighed, frozen in liquid nitrogen, and crushed to a fine powder for the chlorophyll measurements. After extracting the total chlorophyll into 1 mL of 80% acetone and centrifuging for 10 min at 13000 rpm, the amounts of chlorophyll a and b were determined using MacKinney's specific absorption coefficients, with chlorophyll A equaling 12.7(A_{663}) to 2.69(A_{645}) and chlorophyll B equaling 22.9(A_{645}) to 4.48. (A_{663}). The chlorophyll content is expressed as Total chlorophyll/g of seedling tissue.

2.9 | Protein Extraction and Immunoblotting Analysis

Approximately 100 mg of tissue was harvested in a microcentrifuge tube, snap frozen in liquid nitrogen, and ground in 200 μL of protein extraction buffer (50 mM Tris HCl pH 8.0, 150 mM NaCl, 10% glycerol, 5 mM DTT, 1% (v/v) Protease Inhibitor Cocktail, 1% NP40, 0.5 mM PMSF). The protein extract was centrifuged at 10,000 rpm for 15 min to pellet down the debris at 4°C. The supernatant was then transferred to a fresh tube, and an aliquot of 3–5 μL was taken out in a separate tube to estimate protein by Bradford assay reagent (Biorad). The protein samples (1 μg/μl) were boiled for 5–10 min at 100°C.

The denatured protein samples were loaded onto the gel. After separating the protein samples on SDS-PAGE gel, they were transferred to PVDF membrane at 90 V for 1 h in transfer buffer (Tris 48 mM, Glycine 39 mM, 20% methanol pH 9.2) in wet transfer method in the cold room. The membrane was stained with Ponceau-S to confirm the protein transfer and then washed with sterile MQ water. The membrane was then incubated on a rotary shaker for 2 h in 10 mL blocking buffer (5% non-fat dry milk in TBS and 0.05% Tween-20) at room temperature. The blocking reagent was removed, and the affinity-purified primary antibody diluted (1:2000 to 1:10,000) in 10 mL TBS with 0.05% Tween-20 was added and incubated overnight with shaking in a cold room. The membrane was then washed thrice with 10 mL of wash buffer (TBS and 0.05% Tween-20) for 5 min each. The secondary antibody goat anti-mouse (Invitrogen, 31,430), goat anti-rabbit (Abcam, ab205718) HRP conjugated was diluted (1:5000 to 10,000) in 10 mL TBS with 0.05% Tween-20 was added and incubated for 1 h with shaking at room temperature. The membrane was washed thrice with 10 mL of wash buffer at room temperature. Western blot was performed using the Super Signal West Femto chemiluminescent substrate kit (Thermo Scientific, catalog number 34096) and following the manufacturer's instructions. A substrate working solution was prepared by mixing peroxide solution and Luminol/enhancer solution in a 1:1 ratio, and the blot was incubated in that working solution for 5 min in the dark. The blot was then removed from the working solution and observed in Chemi-Doc at different times depending on signal strength. The primary antibodies used in this study were an anti-GFP monoclonal antibody (1:5000 dilution, Takara, 632,592), anti-GFP polyclonal antibody (1:5000 dilution, Abcam, ab290), anti-HY5 antibody (1:2000 dilution, Agrisera, AS12 1867), anti-COP1 antibody (1:2500 dilution, Agrisera, AS20 4399), anti-ubiquitin (1:2000 dilution), Invitrogen, eBioP4D1 (P4D1), and anti-Actin (1:10000 dilution, abcam, ab197345). Goat anti-Rabbit IgG (H + L) Secondary Antibody, HRP (1:10000 dilution, abcam, ab205718), and Goat anti-mouse secondary antibody conjugated to horseradish peroxidase (HRP) (1:5000, Invitrogen, AB_228307) were used as secondary antibodies. For quantitative analysis, the band intensity of HY5 was quantified using ImageJ. Actin was used as the loading control. To measure HY5 protein level, Col-0 was set to 1, and *myc* mutants were compared with it for individual blots. The experiment was repeated at least twice, and a relative protein level was shown.

2.10 | Fluorescence Microscopy

For microscopic analysis, the *35S:MYC3-GFP* transgenic seedlings grown either in constant dark (DD) or DD-grown seedlings treated with WL for 4 h were used. The seedlings were mounted with 10% glycerol in a glass slide. The dark condition was maintained during the sampling procedure. GFP fluorescence signal was visualized by an epifluorescence microscope (Olympus IX81) under 10X magnification with excitation at 480 nm and emission at 535 nm. Photographs of cells expressing GFP were taken for the hypocotyl of each seedling.

2.11 | Bi-Molecular Fluorescence Complementation Assay (BiFC Assay)

For the BiFC studies, full-length CDS of *MYC3* and *MYC4* genes was cloned in pENTR/D-TOPO (Invitrogen, K2400-20) to generate *pENTR-MYC3* and *pENTR-MYC4*. Then, LR Clonase II enzyme mix (Invitrogen, 11,791–020) was used to

generate destination construct in pSPYNE vector to obtain MYC3-YFPN-ter (MYC3-nYFP) and MYC4-YFPN-ter (MYC4-nYFP), respectively. Similarly, full-length CDS of HY5 was cloned in pSPYCE to obtain HY5-YFPC-ter (HY5-cYFP), and full-length CDS of COP1 was cloned in pSPYCE to obtain COP1-YFPC-ter (COP1-cYFP). The constructs and *p19* plasmid were transformed in *Agrobacterium* (GV3101 strain). The assay was performed by following the protocol as described by (Xu et al. 2016) with minor modifications. A single colony of the transformed Agrobacterium was inoculated in 5 mL of YEM media in each case and incubated at 28°C at 200 rpm overnight. The cultures were then centrifuged for 15 min at 4000 g, and the pellets were resuspended in 1 mL of AS medium (100 mM MES-KOH pH 5.6, 100 mM $CaCl_2$, 100 μm acetosyringone). The cell density was diluted with AS medium to OD600 ~ 0.7–0.8. The different Agrobacterium strains harboring the respective constructs were mixed in a ratio of 1:1:0.5 (total volume of 3 mL per leaf) and were allowed to stand for 2–4 h at room temperature. About 200 mL agroinfiltration liquid was slowly injected into the interfaces between the adaxial epidermis and mesophyll of onion bulb scales by using a plastic syringe with a needle, which resulted in an agroinfiltration bubble at the injection spot filled with infiltration liquid occupying about 1 cm^2 area of the epidermis. The fluorescence in the epidermal cell layer expressing the fusion protein was observed after 3 days of infiltration under the fluorescence microscope (Olympus, IX81) at 40X magnification.

2.12 | Co-Immunoprecipitation Assay

For MYC3 Co-IP experiments, Col-0 and *35S:MYC3-GFP* seedlings treated with MG132 were used. For MYC4 Co-IP assays, seedlings of Col-0 and *35S:MYC4-GFP* were not treated with MG132. All the lines were grown in constant dark or light (LD) for 6 days and were used for in vivo protein–protein interaction assay. Approximately 500 μg of total protein of each line were extracted in the buffer containing 50 mM Tris-Cl, pH 8.0, 150 mM NaCl, 10% glycerol, 5 mM DTT, 1% (v/v) protease inhibitor cocktail, 1% NP40, 0.5 mM PMSF and 0.5 mM β-Mercaptoethanol. The assay was performed according to the manufacturer's instructions with minor modifications (Immunoprecipitation Kit-Dynabeads™ Protein G, Invitrogen). The Dynabeads protein G-magnetic beads (Invitrogen; 10007D) and 2.5 μL of anti-GFP polyclonal antibody (Abcam, ab290) were incubated with Ab binding and washing buffer (provided in the kit) overnight at 4°C in the rocker. The next day, the Eppendorf tubes were placed onto a magnetic stand, and the supernatant was discarded. The magnetic bead-Ab-protein complex was resuspended in Ab-binding and washing buffer by gentle pipetting. The extracted protein samples were mixed into the buffer and kept overnight at 4°C. The next day, magnetic beads were separated using a magnetic stand and washed thrice with a washing buffer (provided in the kit). The eluate was collected and boiled at 70°C for 10 min and then run in SDS-PAGE. Both input and IP were analyzed by probing with an anti-HY5 antibody (Agrisera, AS12 1867) and an anti-COP1 antibody (Agrisera, AS20 4399). For checking the protein–protein interaction of MYC3 and MYC4 with COP1, 2.5 μL of anti-COP1 antibody was used for IP reactions, and immunoprecipitated samples were analyzed for the presence of MYC3 or MYC4 using an anti-GFP antibody.

2.13 | Proteasomal Degradation and Ubiquitination Assay

For this experiment, 5-day-old dark-grown seedlings of Col-0, *MYC3-GFP, cop1-4 MYC3-GFP, MYC4-GFP*, and *cop1-4 MYC4-GFP* were treated with MG132 (50 μM *Z-Leu-Leu-Leu-al*, Sigma, C2211) or mock (DMSO) in liquid MS for 16 h. The seedlings were harvested, and total protein was extracted in a protein extraction buffer. The 50 μM MG132 was added to the protein extraction buffer during protein extraction from the treated sample. For the mock samples, DMSO was used in the protein extraction buffer. The boiled protein samples were loaded into SDS-PAGE gel, and a western blot was performed. The co-immunoprecipitation assay was performed by using Dynabeads protein G-magnetic beads (Invitrogen). For IP reactions, an anti-GFP monoclonal antibody (Takara, 632,592) was used. All eluted immunocomplex and input samples were boiled at 70°C for 10 min before immunoblotting. The proteins were analyzed by immunoblotting with anti-ubiquitin (Invitrogen, eBioP4D1 [P4D1], and anti-GFP [Takara, 632592]) antibodies.

2.14 | Sampling of Biological Replicates for Various Assays

For measuring hypocotyl length, at least 20–25 seedlings were used. Three independent biological replicates in combination with three technical replicates were used for gene expression analysis. Six-day-old seedlings were harvested in constant dark (ZT0) or exposed for 4 h in light (WL). The tissue was harvested at ZT4 for real-time qPCR assay. For immunoblot analysis, the 6-day-old seedlings were harvested from LD in WL at diurnal conditions at different Zeitgeber time (ZT) time points. For different monochromatic lights BL, RL, and FRL, including WL and DD under SD conditions, the 6-day-old seedlings were used, and tissue was harvested in ZT4 unless specified otherwise. Col-0 was used as a negative control (ZT4-WL). All experiments were repeated at least twice.

2.15 | Statistical Analysis

Gene expression values were calculated as fold induction relative to Col-0, $n = 3$ (biological), with three technical replicas for each RNA sample. *EF1α* was used as housekeeping gene control. The statistical significance between or among treatments and genotypes was determined based on a one-way analysis of variance or a two-way- analysis of variance test (ANOVA) or Student's *t* test according to the nature of the data. The error bar represents standard deviations.

3 | Results

3.1 | MYC4 Is the Negative Regulator, While Together With MYC3, It Promotes Seedling Photomorphogenesis

To unravel the role of MYC3 and MYC4 in Arabidopsis seedling development, we identified homozygous T-DNA inserted mutant lines for *myc3 (myc3-1)* and *myc4* (*myc4-1)* (Figure S1a,b) and

confirmed that they are null alleles as there was no full-length transcript was detected (Figure S1c,d). The RT-PCR and qRT-PCR also revealed that *myc3* and *myc4* mutants had significantly reduced transcript levels than in Col-0 (Figure S1e–g). We used these alleles for further analysis. Analysis of 6-day-old *myc3* mutants grown under short-day (SD) in white light (WL), blue light (BL), red light (RL), and far-red light (FRL) and in constant dark (DD) showed no defective hypocotyl length compared to wild-type (Col-0) (Figure 1a–j), suggesting that MYC3 does not control hypocotyl growth independently on its own. However, when we analyzed *myc4* mutant, they showed a significant reduction in hypocotyl length in WL and different wavelengths of light (Figure 1a–h) but not in the DD conditions (Figure 1i, j). Notably, *myc4* mutants showed hypersensitive hypocotyl growth under all the light conditions tested (Figure 1a–h), suggesting that MYC4 likely inhibits photomorphogenesis independent of the wavelength of light. We have also examined the hypocotyl length phenotype of different alleles of *myc* mutants *myc2-2*, *myc3-2* and *myc4-2* in 6-day-old seedlings grown in WL under SD photoperiod and found that *myc4-2* has significantly shorter hypocotyls than Col-0 (Figure S2a,b), but *myc2-2* and *myc3-2* hypocotyl length was similar to Col-0 (Figure S2a,b).

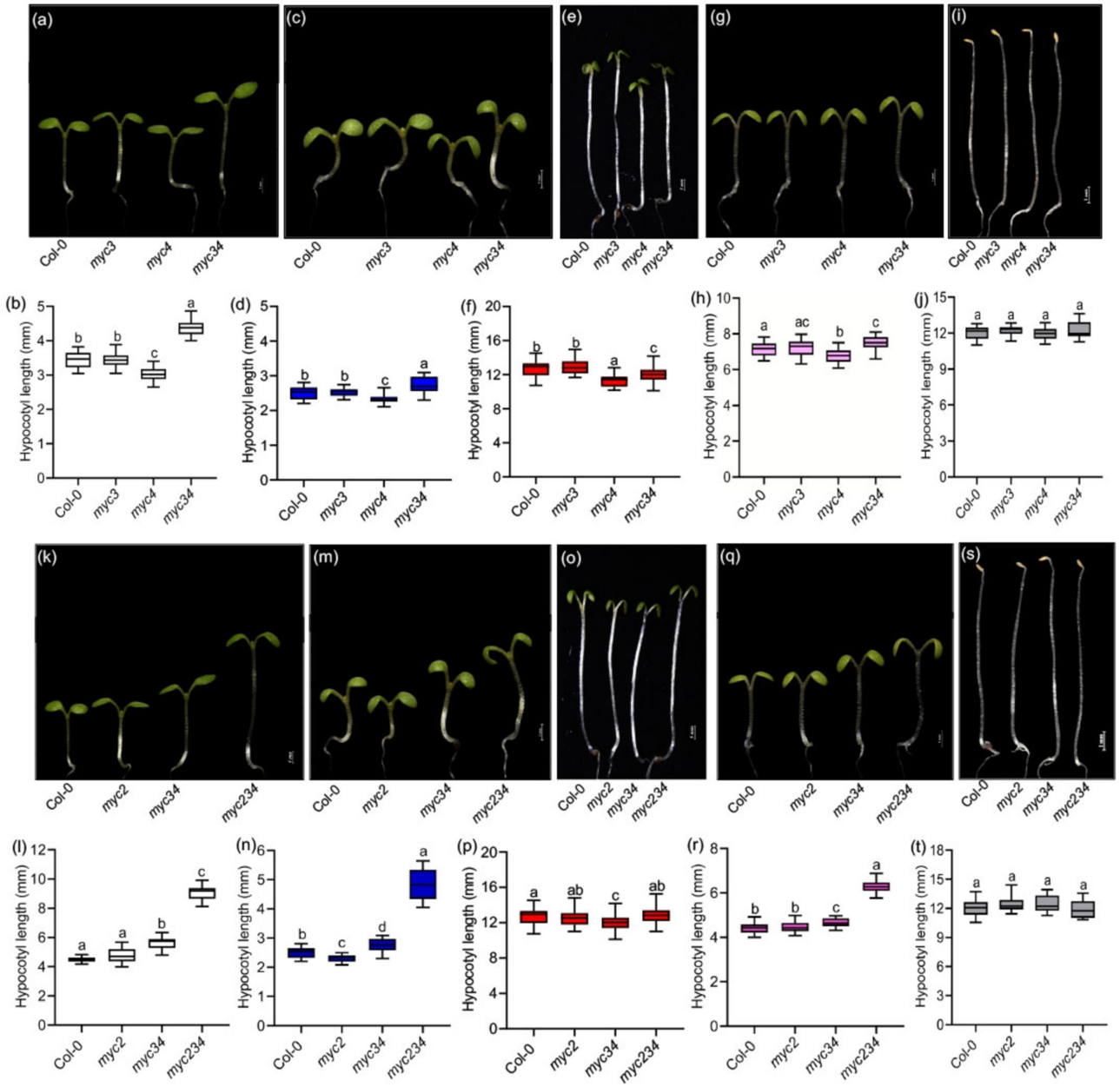

FIGURE 1 | MYC4 inhibits seedling photomorphogenic, while together with MYC3 and MYC2, it strongly enhances photomorphogenic growth. (a–j) Representative seedling images and hypocotyl lengths, respectively, of 6-day-old Col-0, *myc3, myc4, and myc34* double mutant seedlings were grown under 22°C SD in WL (100 μmol m^{-2} s^{-1}) (a and b), BL (35 μmol m^{-2} s^{-1}) (c and d), RL (60 μmol m^{-2} s^{1}) (e and f), FRL (0.5 μmol m^{-2} s^{1}) (g and h), and DD (i and j). (k–t) Representative seedling images and hypocotyl lengths of 6-day-old Col-0, *myc2, myc34,* and *myc234* triple mutant seedlings grown under 22°C SD, respectively, in WL (k and l), BL (m and n), RL (o and p), FRL (q and r), and DD (s and t). Scale Bar = 1 mm. Box-whisker plots represent mean ± SD. Different letters in the box plot indicate a significant difference (one-way ANOVA with Tukey's HSD test, $p < 0.05$, $n \geq 25$ seedlings).

MYCs function partially redundantly and additively in controlling defense responses against herbivores and pathogens and in regulating secondary cell wall thickness (Zhang et al. 2018; Van Moerkercke et al. 2019; Zhang et al. 2020). We wanted to see if MYC3 and MYC4 genetically interact to control seedling hypocotyl growth. We generated a homozygous *myc3myc4* double mutant (hereafter called *myc34*) through a genetic cross and characterized its hypocotyl phenotype to address this. Unexpectedly, *myc34* hypocotyl length was significantly longer than *myc3* and *myc4* and even to Col-0 in WL (Figure 1a,b). Like WL, *myc34* double mutants showed a significant increase in the hypocotyl length compared to *myc4* in BL (Figure 1c,d). However, in RL and FRL, the *myc3myc4* double mutant hypocotyl length was significantly longer than that of the *myc4* mutant, but it was comparable to Col-0 (Figure 1c–h), suggesting that *myc3* mutation can override the effect of *myc4* mutation. In the dark, the *myc34* hypocotyl length was comparable to parental genotypes (Figure 1i,j). We also generated *myc2myc3* (*myc23*) and *myc2myc4* (*myc24*) double mutants by crossing the *myc2*, *jin1-2* allele (Lorenzo et al. 2004) with *myc3* and *myc4*, respectively. When we analyzed *myc23* and *myc24* double mutant hypocotyl lengths in various lights, we found that *myc23* and *myc24* double mutants had hypocotyl lengths taller than Col-0 in WL (Figure S2c,d). However, their length was comparable to Col-0 in BL, RL, FRL and DD (Figure S2e–l). These results imply that even though MYC2 and MYC4 alone function as negative regulators, together with MYC3, they likely act as positive regulators of light-mediated inhibition of seedling hypocotyl growth.

Light differentially controls hypocotyl and cotyledon growth, but the molecular mechanism by which light affects the growth of hypocotyl and cotyledon in plants remains unclear. As MYC3/MYC4 together promote hypocotyl growth inhibition, we wanted to see if they also control cotyledon growth. We examined the cotyledon phenotype of 6-day-old Col-0, *myc3*, *myc4*, and *myc34* seedlings grown in WL and other monochromatic lights under SD photoperiod (Figure S3). Cotyledon area measurement data from 6-day-old seedlings reveal that *myc3* had significantly bigger cotyledons than Col-0 in WL and FRL (Figure S3b,e), while it was comparable to Col-0 in BL and RL (Figure S3c,d). The cotyledon area of the *myc4* mutant was comparable to Col-0 in WL and across different wavelengths of light (Figure S3a–e). Interestingly, the *myc34* mutants had significantly bigger cotyledons than single mutant *myc3*, which has slightly bigger cotyledons than wild-type (Col-0) (Figure S3a–e), suggesting that MYC3/MYC4 functions partially redundantly to inhibit cotyledon expansion. Together, these results indicate that MYC3 and MYC4 differentially control seedling photomorphogenesis in a tissue-specific manner.

3.2 | MYC3/MYC4 Genetically Interact With MYC2 and Together Promote Seedling Photomorphogenesis

Knowing that MYC3 and MYC4 function partially redundantly with MYC2 in controlling defense responses and other aspects of growth and development (Zhang et al. 2018; Van Moerkercke et al. 2019; Zhang et al. 2020), we were intrigued to know the genetic interaction among all three MYCs in seedling photomorphogenic growth. We generated a *myc2myc3myc4* homozygous triple mutant (hereafter called *myc234*) by crossing the *myc34* double mutant with the *myc2* (*jin1-2*) allele (Lorenzo et al. 2004). Measuring the hypocotyl phenotype of 6-day-old seedlings grown in WL under SD photoperiod suggests that, surprisingly, the *myc2/jin1-2* mutation further enhanced the hypocotyl length of the *myc34* double mutant (Figure 1k,l). At the same time, *myc34* showed significantly longer hypocotyls than Col-0, as observed above, while *myc2* mutant hypocotyl length was comparable to Col-0 under SD (Figure 1k,l). Like WL, the *myc234* triple mutant showed significantly elongated hypocotyl than the *myc34* double mutant under BL (Figure 1m,n). The elongated hypocotyl length of the *myc234* triple mutant is also consistent with the earlier reports, specifically under long-day photoperiod or constant light (Chico et al. 2014; Ortigosa et al. 2020). However, as reported, *myc2* showed significantly shorter hypocotyl than Col-0 in BL (Figure 1m,n). In RL, the triple mutant hypocotyl length was largely comparable to Col-0 (Figure 1o,p), while in FRL, it showed significantly longer hypocotyls than the double mutants and Col-0 (Figure 1q,r). In DD, the *myc234* triple mutant hypocotyl length was similar to parental genotypes (Figure 1s,t). These results reveal that MYC3/MYC4 interact with MYC2 and exhibit unequal genetic redundancy to inhibit light-mediated seedling hypocotyl growth.

3.3 | MYC2/MYC3/MYC4 Together Regulate Anthocyanin and Chlorophyll Accumulation

Besides inhibiting hypocotyl growth, seedling photomorphogenesis also accompanies an increased accumulation of photopigments such as anthocyanin and chlorophyll. As *myc234* triple mutants showed a strong light-insensitive response to hypocotyl growth inhibition, we wanted to know if the accumulation of photopigments is also altered. Analysis of anthocyanin content from 6-day-old seedlings revealed that *myc2* and *myc4* accumulated slightly but significantly more anthocyanin in WL, BL, and RL (Figure S4a–c); however, the *myc3* mutant accumulated slightly more anthocyanin in RL but not in other light conditions (Figure S4c). The anthocyanin content in the *myc34* double mutants is largely comparable to Col-0 (Figure S4a–d). Interestingly, consistent with the reduced light sensitivity of the *myc234* triple mutant, their anthocyanin content was significantly reduced than Col-0 in WL and different wavelengths of light (Figure S4a–d), suggesting that MYC2/MYC3/MYC4 together act to promote anthocyanin accumulation. Unlike anthocyanin accumulation, the triple mutants had significantly less chlorophyll content in WL and RL (Figure S4e,f) but not in BL and FRL (Figure S4g,h). The chlorophyll content of *myc34* was largely similar to Col-0 in WL and other wavelengths of light (Figure S4e–h). However, the *myc2* and *myc4* mutants accumulated significantly more chlorophyll than Col-0 in WL, BL, and RL (Figure S4e–g) but not in FRL (Figure S4h). These data suggest that MYC2/MYC3/MYC4 differentially regulate chlorophyll and anthocyanin accumulation in a wavelength-dependent manner.

3.4 | MYC2/MYC3/MYC4 Modulates the Expression of Light-Inducible Genes

MYC2 has been shown to inhibit the expression of light-inducible genes such as *CHLOROPHYLL A/B BINDING 1*

(*CAB1*), *RIBULOSE BISPHOSPHATE CARBOXYLASE SMALL SUBUNIT-1A (RBCS-1A*) and *EARLY LIGHT-INDUCIBLE PROTEIN 2* (*ELIP2*), involved in the photosynthetic reaction; and *CHALCONE SYNTHASE* (*CHS*) and *CHALCONE ISOMERASE* (*CHI*), which code for enzymes involved in anthocyanin biosynthesis (Yadav et al. 2005). We are curious to know how *MYCs* individually and together control the expression of light-inducible genes. Our qRT-PCR data revealed that the expression of these genes is significantly reduced in the *myc234* triple mutant than Col-0 when constant dark-grown seedlings were exposed to light for 4 h (Figure 2a–f). Consistent with reduced anthocyanin and chlorophyll accumulatio, the *myc234* triple mutants showed compromised expression of various light-inducible genes such as *CAB1*, *RBCS-1A, ELIP2, CHS* and *CHI* (Figure 2a–e). Moreover, the key transcription factor *HY5*, which directly binds and activates *CAB1*, *RBCS-1A*, *ELIP2*, *CHS*, and *CHI* (Ang et al. 1998; Chattopadhyay et al. 1998; Catalá, Medina, and Salinas 2011; Hayami et al. 2015), showed significant downregulation in the *myc234* triple mutant than Col-0 (Figure 2f), suggesting that reduced expression of these genes in the *myc234* triple mutant is likely due to reduced *HY5* expression. In the *myc34* double mutants, the expression of these genes is largely comparable to Col-0 (Figure 2a–e). Interestingly, the expression of *CAB1*, *RBCA-1A*, *ELIP2*, *CHS* and *CHI* genes was significantly elevated in the *myc2* mutant than Col-0 (Figure 2a–e), while in *myc4* it was largely similar to Col-0 in 4-h light-treated seedlings (Figure 2a–e). Notably, genes such as *ELIP2*, *CHS*, and *CHI* showed significant upregulation in the *myc3 and myc4* single mutants compared to Col-0 in the dark (Figure 2c–e). Together, these data suggest that MYCs differentially regulate the expression of light-inducible genes.

3.5 | Light Regulates MYC4 Gene Expression and Protein Accumulation

As MYC3 and MYC4 regulate seedling photomorphogenic growth, we wanted to know if light regulates their gene expression and protein accumulation. We carried out our qRT-PCR analysis from 6-day-old seedlings under SD conditions (ZT3) and found that both *MYC3* and *MYC4* gene expression is significantly upregulated in WL, BL, RL, and FRL compared to constant dark-grown seedlings (Figure S5a), suggesting that MYC3/MYC4 gene expression is elevated under light conditions than dark. Also, when we analyzed their gene expression in different tissues, we found that *MYC3* and *MYC4* ubiquitously expressed across different tissue types (Figure S5b).

Next, to check if light regulates their protein accumulation, we performed immunoblot assays using *35S:MYC3-GFP* and *35S:MYC4-GFP* transgenic lines (Fernandez-Calvo et al. 2011), which express significantly increased transcript levels than the Col-0 (Figure S6a,b). Immunoblotting data revealed that MYC4 protein accumulated more in light conditions such as WL-grown SD, LD, and LL photoperiods than in DD (Figure 3a). Compared to SD, LD-grown seedlings accumulated slightly more MYC4 protein, while constant light (LL) grown seedlings accumulated a similar protein level to SD (Figure 3a). Similarly, when DD-grown seedlings

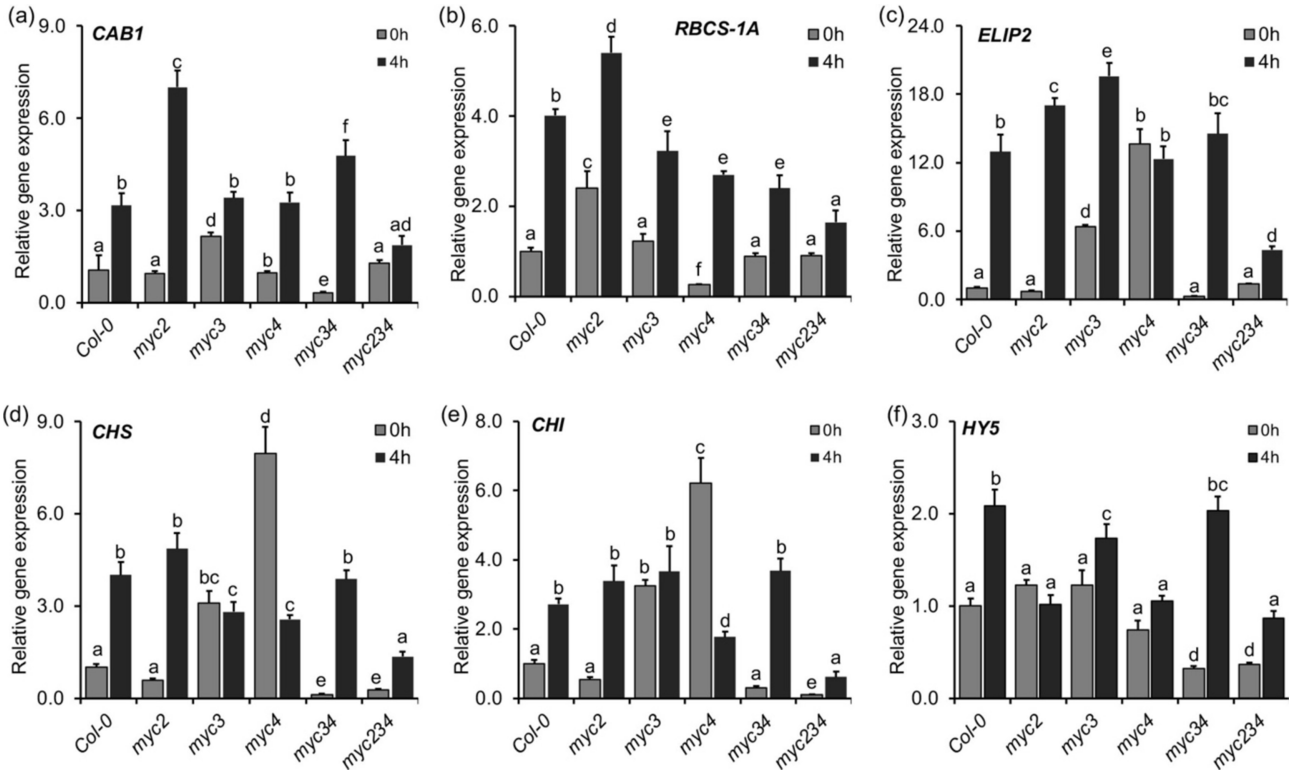

FIGURE 2 | Expression of light-inducible genes in various *myc* mutants. (a–f) Expression of light-inducible genes *CAB1* (a), *RBCS-1A* (b), *ELIP2* (c), *CHS* (d), *CHI* (e), and *HY5* (f) in 6-day-old seedlings of Col-0, *myc2, myc3, myc4, myc34,* and *myc234* grown in constant dark for 6 days and 4-h WL (100 μmol m^{-2} s^{-1}) treated seedlings. The bars represent the mean ± SD (n = three biological replicates). The data were first normalized with *EF1α* and then calculated fold-change against wild-type 0 h as 1. Different letters above the bars indicate a significant difference from other genotypes or treatments (two-way ANOVA with Tukey's HSD test, $p < 0.05$, $n = 3$).

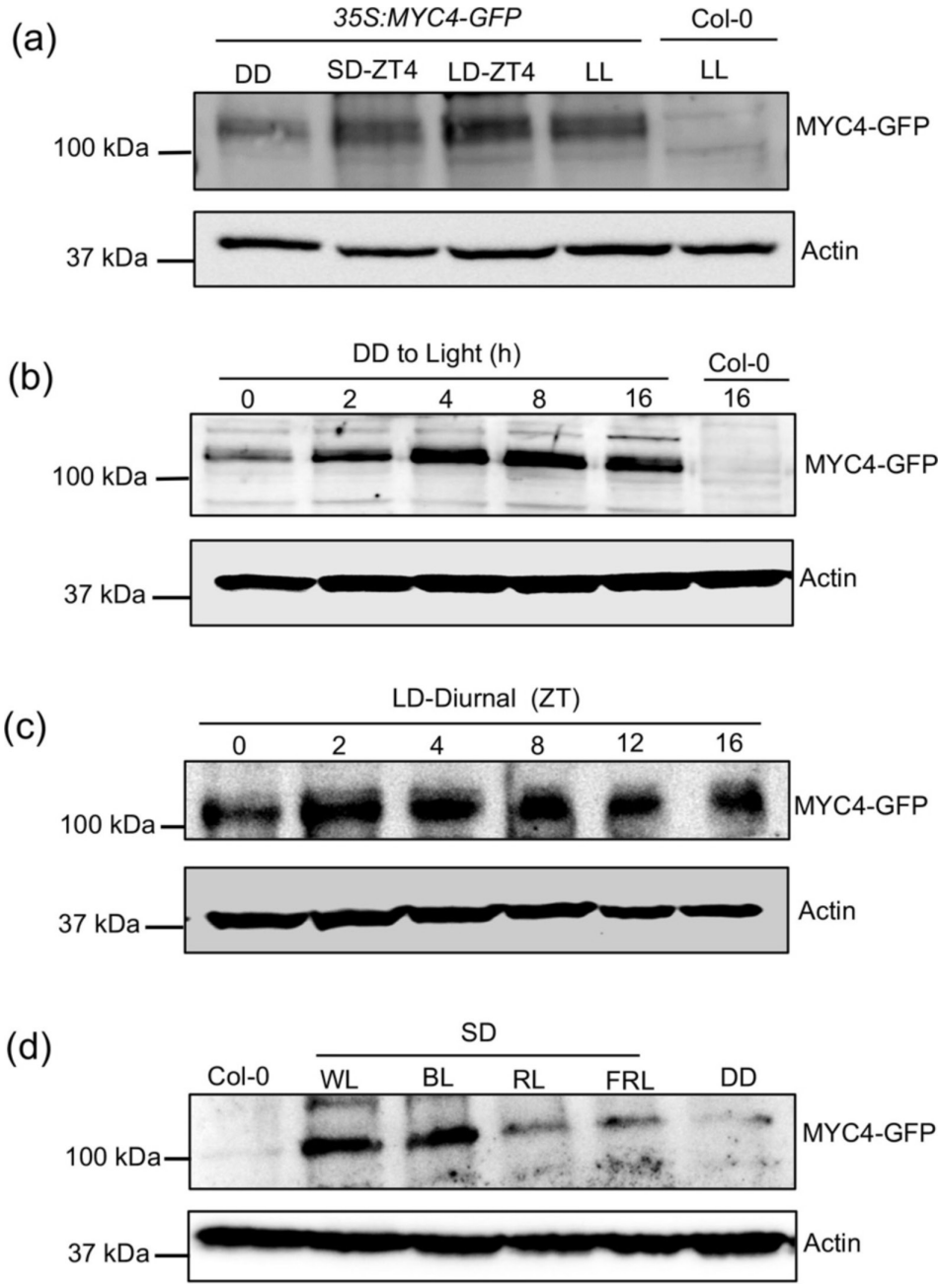

FIGURE 3 | Light regulates MYC4 protein accumulation. (a) Immunoblot analysis from 6-day-old seedlings of *35S:MYC4-GFP* transgenic line in constant dark (DD), SD (ZT4), LD (ZT4), and constant light (LL). The light intensity of 100 μmol m^{-2} s^{-1} was used. (b) Immunoblot analysis of *35S:MYC4-GFP* transgenic line. Six-day-old DD-grown seedlings were shown at 0 h and then treated with WL for different time duration as indicated. (c) Immunoblot analysis of 6-day-old seedlings of *35S:MYC4-GFP* line grown in WL under LD photoperiods for different time periods as indicated. (d) Immunoblot of *35S:MYC4-GFP* seedlings grown under different monochromatic lights BL (35 μmol m^{-2} s^{-1}), RL (60 μmol m^{-2} s^{1}), and FRL (0.5 μmol m^{-2} s^{1}), including WL under SD (tissue harvested at ZT4) and DD. In Panels (a), (b), and (d), Col-0 seedlings were used as a negative control. The total protein was extracted and then subjected to immunoblot analysis using an anti-GFP antibody. The MYC4-GFP is shown as indicated. The lower panels show the immunoblot of anti-Actin as loading controls.

were shifted to WL for different durations, light-treated seedlings accumulated more MYC4 protein than the DD-grown seedlings (Figure 3b). Moreover, under diurnal LD conditions, compared to ZT0, MYC4 protein stability was higher during the daytime (ZT2-ZT8) and started declining at the end of the day (ZT12-ZT16) (Figure 3c). Besides, when we checked the MYC4 protein levels under different wavelengths of light, we found that MYC4 protein accumulated more in WL and BL than in RL, FRL, and DD (Figure 3d). Together, these results reveal that light promotes MYC4 protein accumulation. Further, we checked the protein levels of MYC3 using *35S:MYC3-GFP* transgenic line (Fernandez-Calvo et al. 2011). Unlike MYC4, we could not detect MYC3 protein under any tested conditions, including different wavelengths and photoperiods (Figure S6c–f), suggesting that MYC3 protein is probably highly unstable. However, when we analyzed 5-day-old dark-grown *35S:MYC3-GFP* seedlings under the fluorescent

microscope, we could detect weak *MYC3-GFP* fluorescence in the hypocotyl cells but not in the wild-type (Col-0) that was used as a negative control (Figure S6g). Notably, the MYC3-GFP fluorescence was slightly higher in seedlings treated with light than the DD gown seedlings (Figure S6g), indicating that MYC3 protein stability could be under the regulation of E3 ubiquitin ligase(s) to control its function.

3.6 | MYC3 and MYC4 Regulate Petiole and Rosette Development

To further know if MYC3 and MYC4 influence growth beyond seedling development, we examined their rosette and petiole phenotypes. The *myc3* mutant had a similar rosette size to Col-0, while *myc4* had significantly smaller rosettes than Col-0 under SD and LD photoperiods (Figure S7a–c). Interestingly, the *myc34* double mutants had slightly but significantly increased rosette diameter under SD and LD (Figure S7a–c).

In line with the increased rosette diameter, the *myc3* mutant had petiole length similar to Col-0, while *myc4* had significantly shorter petioles (Figure S7d,e). However, the petiole length of *myc34* double mutants was significantly longer than the parental genotypes and Col-0 under both SD and LD photoperiods (Figure S7d,e). These results are also consistent with the earlier report of increased petiole length in the *myc34* double mutant (Li, Nozue, and Maloof 2020). These results suggest that similar to regulating hypocotyl growth, MYC3/MYC4 likely exhibits unequal redundancy in regulating rosette and petiole growth and development.

3.7 | MYC3 and MYC4 Genetically Interact With HY5 and Suppress Its Function

HY5, a potent activator of seedling photomorphogenesis, functions downstream to all the known photoreceptors (Oyama, Shimura, and Okada 1997; Chattopadhyay et al. 1998). We were interested to see if MYC3 and MYC4 genetically interact with HY5 in regulating seedling hypocotyl growth. We generated *myc3hy5* and *myc4hy5* double mutants and investigated their phenotypes. Measurement of hypocotyl lengths revealed that *hy5* showed long and partially etiolated hypocotyls in WL compared to Col-0, as reported (Ang and Deng 1994; Chattopadhyay et al. 1998) (Figure 4a,b). However, *myc3* and *myc4* mutations significantly suppressed the *hy5* hypocotyl phenotype as the hypocotyl length of *myc3hy5* and *myc4hy5* was significantly reduced than *hy5* (Figure 4a,b). Similarly, *myc3hy5* and *myc4hy5* double mutants displayed significantly shorter hypocotyls than *hy5* in BL, RL, and FRL conditions (Figure 4c–h), suggesting that MYC3 and MYC4 genetically interact with HY5 and probably function antagonistically to control hypocotyl growth. The suppression of *hy5* mutant hypocotyl length by *myc3* and *myc4* is also consistent with the genetic interaction observed for MYC2 and HY5 (Chakraborty et al. 2019), wherein *myc2* could strongly suppress the long hypocotyl phenotype of *hy5*. Consistent with the unequal genetic redundancy observed in *myc34* double mutants, we tested the effect of *myc34* mutations together in modulating *hy5* mutant hypocotyl growth. We generated a *myc3myc4hy5* (*myc34hy5*) triple mutant and measured hypocotyl length in WL and different monochromatic lights. Our data revealed that the hypocotyl length of the *myc34hy5* triple mutant was slightly but significantly longer than the *myc3hy5* and *myc4hy5* double mutants (Figure 4a–h), suggesting that when both MYC3 and MYC4 are absent, their ability to suppress *hy5* hypocotyl phenotype is reduced than when any one of them is absent.

Similar to the effect seen in controlling hypocotyl growth, *myc3* and *myc4* mutations also significantly suppressed low anthocyanin levels of *hy5* in WL and BL (Figure 4i,j). However, in the *myc34hy5* triple mutant, anthocyanin levels were comparable to *hy5* (Figure 4i,j). In RL, anthocyanin levels in the *myc3hy5*, *myc4hy5* and *myc34hy5* were largely similar to the *hy5* mutant (Figure 4k). In FRL, the anthocyanin levels in the *myc3hy5* and *myc4hy5* were comparable to *hy5*, while it is further reduced than *hy5* in the *myc34hy5* triple mutants (Figure 4l). Similarly, *myc3hy5*, *myc4hy5*, and *myc34hy5* accumulated chlorophyll content similar to *hy5* in all the light conditions, including WL (Figure 4m–p). However, *myc34* suppressed the low chlorophyll content of *hy5* in WL and RL but not in BL and FRL (Figure 4m–p), further suggesting that MYC3 and MYC4 probably influence HY5 function differentially in a light-dependent manner to regulate anthocyanin and chlorophyll accumulation.

3.8 | MYCs Activity Is Essential for the Optimal Accumulation of HY5 Protein

As MYCs modulate HY5-mediated hypocotyl growth and regulate *HY5* gene expression, we were curious to know if they also regulate HY5 protein levels. We carried out immunoblotting assays using HY5-specific native antibodies (Figure S8). Six-day-old seedlings grown in WL under SD revealed that in *myc2*, *myc3, myc4* single, and *myc34* double mutant, HY5 protein levels were comparable to Col-0 (Figure 5a,b). However, in the *myc234* triple mutant, the HY5 protein levels were markedly reduced compared to Col-0 (Figure 5a,b). Under WL-LD, HY5 protein levels was reduced in the *myc234* triple mutants (Figure 5c,d) but not in the single and double mutants of *MYCs*, suggesting that MYC2/MYC3/MYC4 play a key role in maintaining optimal HY5 protein levels. In BL-grown seedlings, we saw a moderate reduction in the HY5 protein levels in the *myc234* mutants compared to Col-0 (Figure 5e,f). However, the HY5 protein levels in *myc* single and *myc34* double mutant was comparable to Col-0 (Figure 5e,f). Similarly, in the RL, HY5 protein accumulation was reduced in the *myc234* triple mutant but not in the single and double mutants of *mycs*, compared to Col-0 (Figure 5g,h). In FRL conditions, the *myc234* and *myc34* mutants showed reduced HY5 protein accumulation compared to Col-0, whereas the *myc* single mutants showed similar HY5 protein levels to Col-0 (Figure 5i,j). These data suggest that MYC2/MYC3/MYC4 differentially regulate endogenous HY5 protein accumulation in a light wavelength-dependent manner.

3.9 | MYC3/MYC4 Physically Interact With HY5

As MYC3 and MYC4 genetically interact and regulate HY5 protein stability to control seedling photomorphogenic growth, we wanted to check if MYC3/MYC4 physically interacts with HY5 and regulates its function and protein stability. To address this, we performed an In vivo co-immunoprecipitation assay using

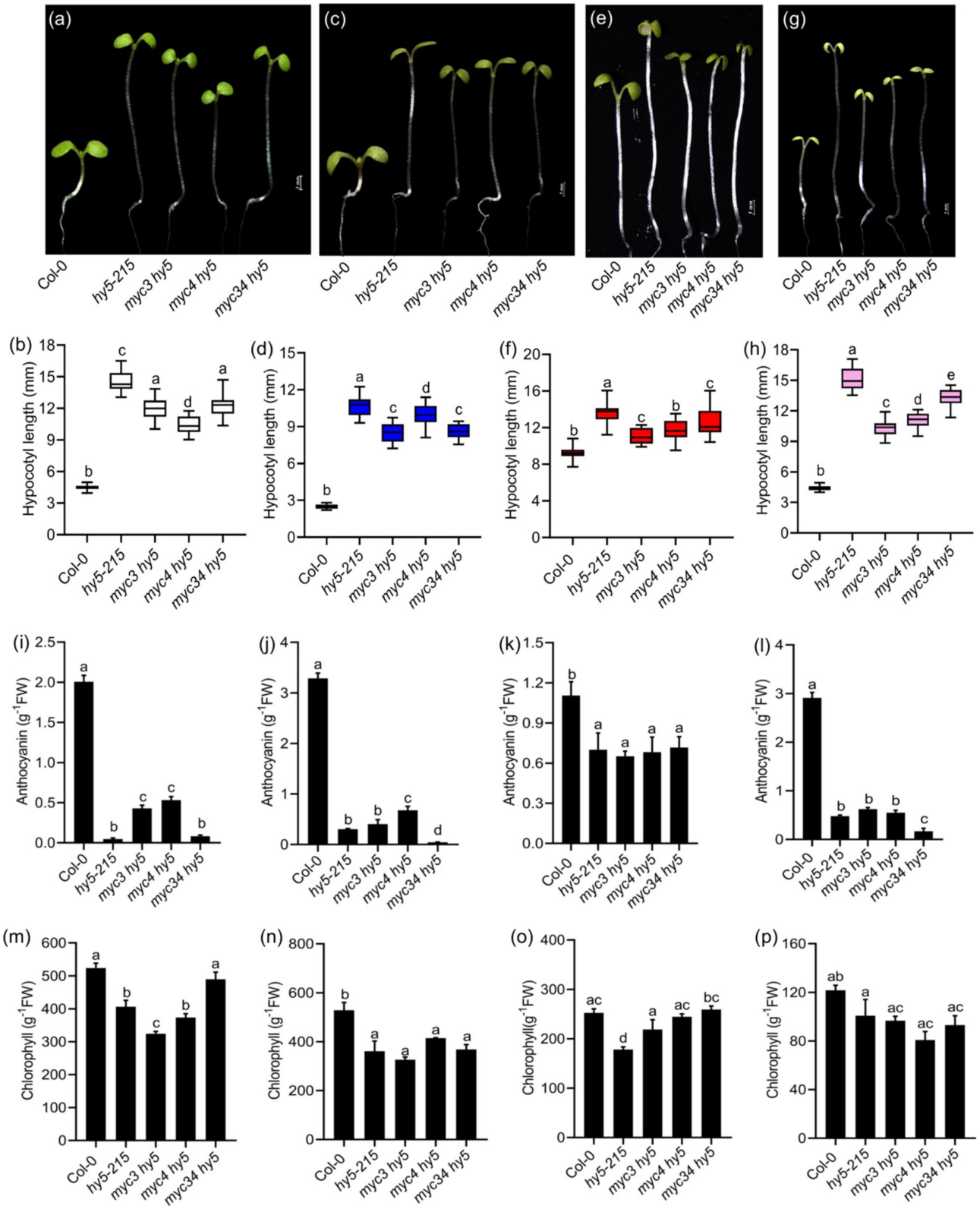

FIGURE 4 | MYC3/MYC4 genetically interacts with HY5 to regulate seedling photomorphogenic growth. (a–h) Representative seedling pictures and the hypocotyl length of 6-day-old Col-0, *hy5–215, myc3hy5, myc4hy5,* and *myc34 hy5* triple mutant seedlings grown in WL ($100\,\mu mol\,m^{-2}s^{-1}$) (a and b), BL ($35\,\mu mol\,m^{-2}s^{-1}$) (c and d), RL ($60\,\mu mol\,m^{-2}s^{1}$) (e and f), and FRL ($0.5\,\mu mol\,m^{-2}s^{1}$) (g and h) under SD photoperiod. The data shown is mean ± SD, ≥25 seedlings. (i–l) Quantification of anthocyanin content in the indicated genotypes shown grown in SD photoperiod for 6 days in WL (i), BL(j), RL (k), and FRL (l). The seedlings were harvested at ZT23. The data shown is mean ± SD, ≥20 seedlings (m–p) Chlorophyll content of 6-day-old seedlings of mentioned genotypes grown in WL (m), BL(n), RL(o), and FRL (p) conditions under SD. The tissue for the experiment was harvested at ZT23. The data shown is mean ± SD, ≥20 seedlings. Different letters above the bar chart indicate a significant difference (one-way ANOVA with Tukey's HSD test, $p < 0.05$).

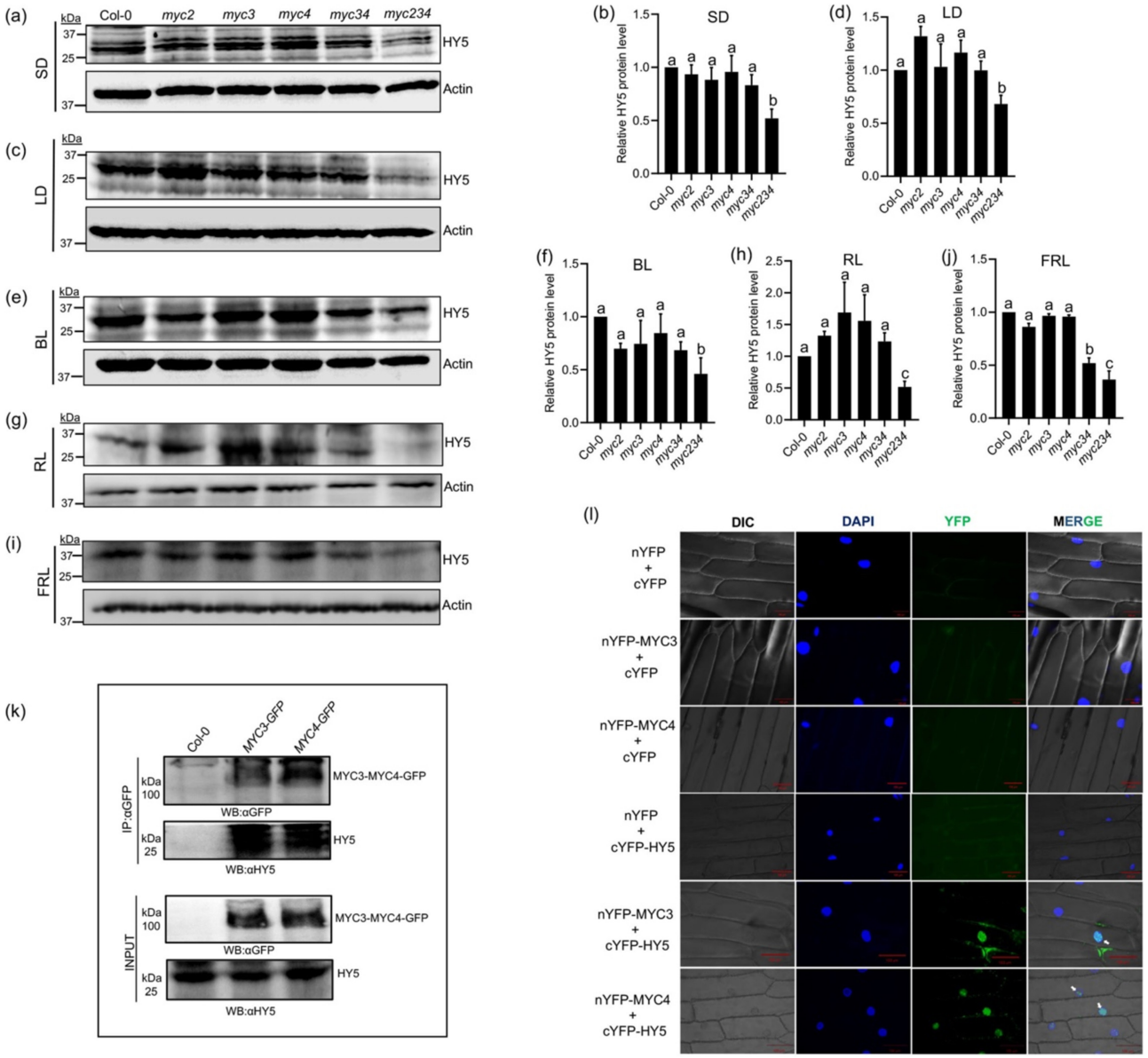

FIGURE 5 | MYC2/MYC3/MYC4 regulate HY5 protein accumulation, probably through physical interaction. (a–j) Immunoblot to detect HY5 protein levels using native HY5 protein antibody in 6-day-old seedlings of Col-0, *myc2, myc3, myc4, myc34*, and *myc234* triple mutant grown in WL under SD (a and b) and LD (c and d); and under SD in BL ($35\,\mu mol\,m^{-2}s^{-1}$) (e and f), RL ($60\,\mu mol\,m^{-2}s^{1}$) (g and h), and FRL ($0.5\,\mu mol\,m^{-2}s^{1}$) (I and j). The tissue was harvested at ZT4. For the WL experiment, the light intensity of $100\,\mu mol\,m^{-2}s^{-1}$ was used for both SD and LD conditions. Actin blots were shown for loading control. The relative protein levels of HY5 from two independent experiments were shown for the various conditions as indicated. Actin was used as a loading control and was also used for normalization for each immunoblot. Different letters above the bar chart indicate a significant difference (one-way ANOVA with Tukey's HSD test, $p < 0.05$). (k) Immunoblot showing coimmunoprecipitation of HY5 when MYC3-GFP or MYC4-GFP proteins were immunoprecipitated using an anti-GFP antibody. The *35S:MYC3-GFP* and *35S:MYC4-GFP* transgenic lines grown in WL ($100\,\mu mol\,m^{-2}s^{-1}$) under LD for 6 days were used. As MYC3 is not detectable, *35S:MYC3-GFP* seedlings treated with MG132-treated were used for the assay. The immunoprecipitated complex was resolved by SDS-PAGE. Both the input and IP were probed with antibodies to HY5. The tissue harvested at ZT4 was used for Co-IP assays. Wild type (Col-0) was used as a negative control for the GFP line. (l) BiFC assay suggests physical interaction between MYC3/MYC4 and HY5. All the constructs containing nYFP and cYFP were co-transformed into onion epidermal cells. nYFP-MYC3/cYFP-HY5 and nYFP-MYC4/cYFP-HY5 combination show positive signals for interactions. The left panel image shows the bright field image (DIC), the middle panel shows the nucleus staining by DAPI, and the next panel shows the YFP channel produced by the reconstruction of YFP by using Olympus IX81 at 40X magnification. The right panel image shows the merged image. Scale Bars = 100 μm. The Arrows indicate the reconstituted YFP signal in the nuclei.

6-day-old *35S:MYC3-GFP* seedlings treated with proteasome inhibitor MG132 (as *MYC3-GFP* was not stable under the conditions tested) and *35S:MYC4-GFP* transgenic lines grown in WL under LD. Our immunoblot data show that when either MYC3-GFP or MYC4-GFP was immunoprecipitated using an anti-GFP antibody, we could detect HY5 protein being pulled down in immunoprecipitated complex along with MYC3-GFP and MYC4-GFP, as detected using an anti-HY5 antibody (Figure 5k). However, when we used Col-0 as a negative control, HY5 protein was not detectable in the immunoprecipitated complex

(Figure 5k), suggesting that HY5 could physically associate with MYC3 and MYC4. These results were further confirmed by BiFC assay in the onion epidermal cells. When cYFP-HY5 was co-infiltrated with either nYFP-MYC3 or nYFP-MYC4, we could detect a YFP fluorescence in the nucleus, as revealed by microscopy (Figure 5l). However, we could not detect fluorescence when cYFP-HY5/nYFP, cYFP/nYFP-MYC3, cYFP/nYFP-MYC4, or nYFP/cYFP combinations were co-infiltrated (Figure 5l), indicating that MYC3/MYC4 physically interacts with HY5.

3.10 | MYC3 and MYC4 Genetically Interact With COP1 and Modulate Its Function

COP1 is a critical repressor of the photomorphogenesis (Deng, Caspar, and Quail 1991). It ubiquitinates and degrades many positive regulators of seedling photomorphogenesis, such as HY5, HYH, LAF1, HFR1, and BBX proteins (Osterlund et al. 2000; Holm et al. 2002; Seo et al. 2004; Lau and Deng 2012). An earlier study showed that the *myc2* (*jin1-2*), *myc3-1*, and *myc234* mutants harbor a hidden mutation in the *COP1* gene (Yu et al. 2023), leading to a missense mutation in the seventh WD-repeat domain of COP1, which subsequently induces early flowering in these mutants. We wanted to see if our *myc* also contained this hidden mutation in the *COP1* gene. Extraction of genomic DNA followed by genotyping with dCAPs revealed the presence of *cop1-21* mutation [guanine (G) to adenine (A) substitution] in the *myc2* (*jin1-2*) and *myc234* triple mutant (Yu et al. 2023), which has the *myc2* (*jin1-2*) (Figure S9). However, the *myc3-1*, *myc4-1* and *myc34* double mutants did not contain the *cop1-21* mutation, suggesting that only the *jin1-2* allele harbors the *cop1-21* mutation in the *COP1* gene.

As MYC2 has been shown to genetically interact with COP1 (Zheng et al. 2017), we wanted to see the epistatic interactions of MYC3 and MYC4 with COP1, so we generated *myc3cop1-4* and *myc4cop1-4* double mutants and *myc3myc4cop1-4* triple mutants and analyzed their hypocotyl phenotype. Measurement of hypocotyl length from 6-day-old constant dark-grown (DD) seedlings revealed that *myc3cop1-4* had hypocotyl length largely similar to the *cop1-4* single mutant, while *myc4cop1-4* had subtle but significantly shorter hypocotyls than *cop1-4* (Figure 6a,b). Similarly, the *myc34cop1-4* triple mutant hypocotyl length was significantly shorter than *cop1-4* but comparable to the

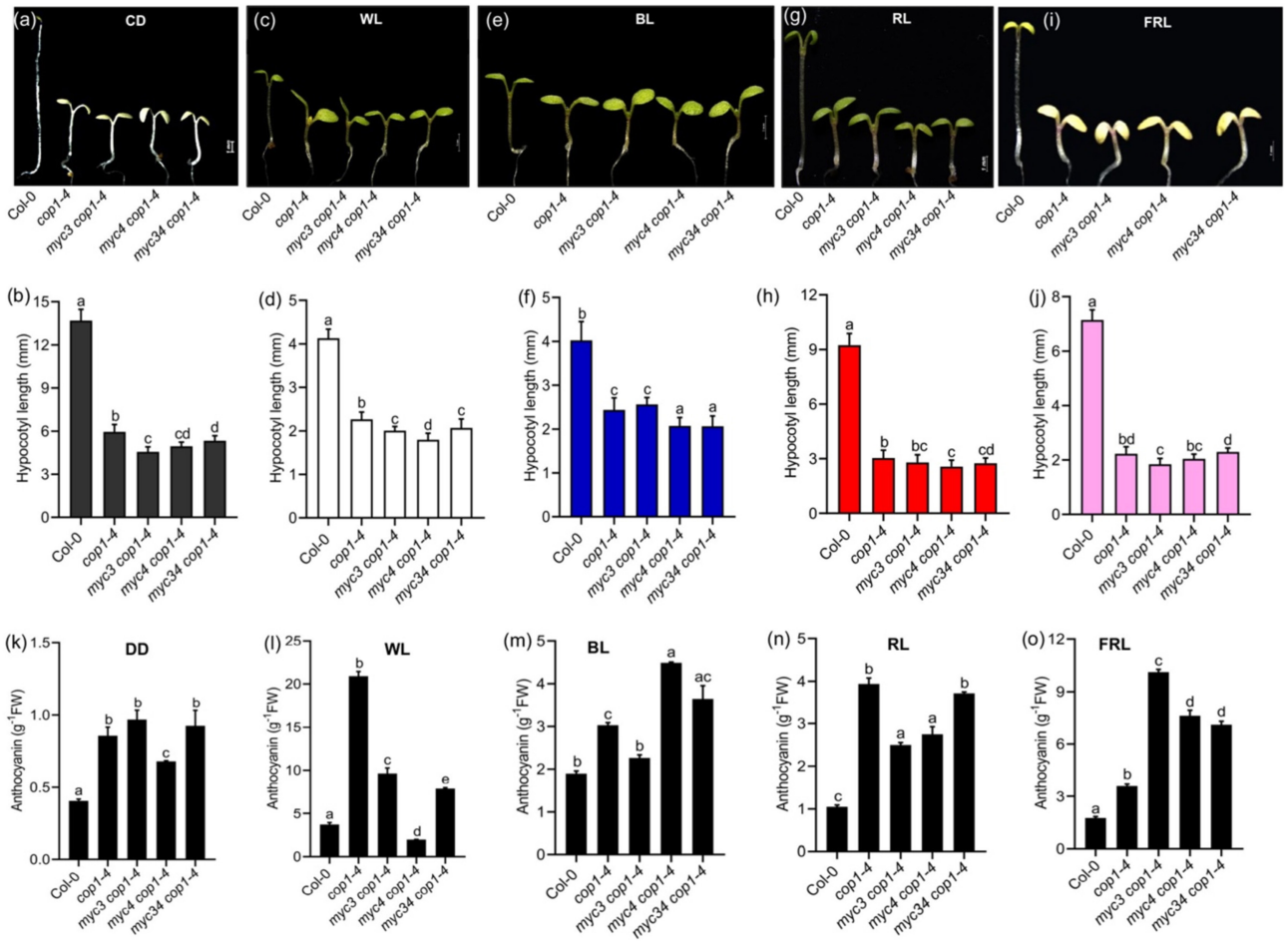

FIGURE 6 | Genetic interaction between MYC3/MYC4 and COP1 to control regulation of photomorphogenesis.(a–j) Representative seedling images and measured hypocotyl length of Col-0, *cop1-4*, *myc3cop1-4, myc4cop1-4,* and *myc34cop1-4* mutant seedlings grown for 6 days in constant dark DD (a and b); and under SD photoperiod in WL (100 μmol m^{-2} s^{-1}) (c and d), BL (35 μmol m^{-2} s^{-1}) (e and f), RL (60 μmol m^{-2} s^{-1}) (g and h), and FRL (0.5 μmol m^{-2} s^{1}) (i and j). Scale bar = 1 mm. The data shown is mean ± SD, ≥25 seedlings (k–o) Anthocyanin contents in the indicated genotypes grown in SD photoperiod for 6 days in constant dark (k) and under SD in WL (l), BL (m), RL (n), and FRL (o). The data shown is mean ± SD, ≥20 seedlings. Different letters above the bar chart indicate a significant difference (one-way ANOVA with Tukey's HSD test, $p < 0.05$).

myc4cop1-4 double mutant (Figure 6a,b). Like DD, 6-day-old WL-grown *myc3cop1-4 and myc4cop1-4* seedlings under SD photoperiod had significantly shorter hypocotyls than *cop1-4*, while the *myc34cop1-4* triple mutant hypocotyl length was comparable to the *myc3cop1-4* double mutant (Figure 6c,d). In BL, *myc3cop1-4* hypocotyl length was comparable to *cop1-4*, while the *myc4cop1-4* and *myc34cop1-4* had significantly shorter hypocotyls than *cop1-4* (Figure 6e,f). Under RL, the hypocotyl length of *myc4cop1-4* and *myc34cop1-4* was significantly shorter than the *cop1-4*, while that of *myc3cop1-4* was comparable to *cop1-4* (Figure 6g,h). In FRL, the *myc3cop1-4* had significantly shorter hypocotyls than *cop1-4*, while *myc4cop1-4* and *myc34cop1-4* hypocotyl length was comparable to *cop1-4* (Figure 6i,j). These results indicated that MYC3 and MYC4 likely enhance COP1 function to promote hypocotyl elongation in dark and light.

3.11 | MYC3 and MYC4 Regulate COP1-Mediated Anthocyanin Accumulation in Dark and Light

The various alleles of *cop1* mutant accumulate elevated anthocyanin in addition to suppressing hypocotyl growth (Deng, Caspar, and Quail 1991; Ang and Deng 1994). To know if MYC3 and MYC4 interfere with COP1 in controlling anthocyanin accumulation, we quantified anthocyanin content in DD, WL, and different nonchromatic light-grown seedlings. As expected, the anthocyanin content in *cop1-4* was significantly higher than that of Col-0 in DD. The *myc3cop1-4* and *myc34cop1-4* mutants were comparable to *cop1-4* (Figure 6k). However, in the *myc4cop1-4*, anthocyanin levels are slightly lower than *cop1-4* but significantly more than Col-0 (Figure 6k). In WL-SD-grown seedlings, *cop1-4* accumulated significantly more anthocyanin than Col-0 (Figure 6l). However, in the *myc3cop1-4, myc4cop1-4*, and triple mutants, anthocyanin content was significantly reduced than *cop1-4* (Figure 6l). However, in BL, the anthocyanin content of *myc4cop1-4* and *myc34cop1-4* was significantly elevated compared to that of *cop1-4*, while it was similar to Col-0 (Figure 6m). In the RL, anthocyanin content in *myc3cop1-4, myc4cop1-4*, and *myc34cop1-4* mutants was significantly elevated than the *cop1-4*. However, in the triple mutant, there was more than in both the single mutants (Figure 6n). Like BL, the anthocyanin content *cop1-4* was further enhanced in double and triple mutants under FRL (Figure 6o).

While COP1 is a negative regulator of anthocyanin in the dark and across different wavelengths of light, it differentially regulates chlorophyll accumulation in a light and allele-specific manner. In WL and FRL, *cop1-4* accumulates less chlorophyll than Col-0, while the *myc3cop1-4, myc4cop1-4* double and *myc34cop1-4* triple mutants had similar chlorophyll levels to *cop1-4* (Figure S10a,d). In BL, *cop1-4* accumulated more chlorophyll than Col-0, while *myc3myc4* further enhanced the chlorophyll content of the *cop1-4* mutant (Figure S10b). Like BL, *cop1-4* accumulates more chlorophyll in RL than Col-0 (Figure S10c). However, in the *myc3cop1-4, myc4cop1-4* double and *myc34cop1-4* triple mutant, it was comparable to *cop1-4* (Figure S10b), suggesting that MYC3 and MYC4 interaction with COP1 for the regulation of anthocyanin and chlorophyll is dependent on wavelength of light. Together, these results conclude that varying phenotypic outputs seen among *myc3cop1-4, myc4cop1-4* double, and *myc34cop1-4* triple mutants are likely due to the unequal genetic redundancy observed between MYC3 and MYC4, but not due to the presence of *cop1-21* mutation.

3.12 | MYC3/4 Interferes With COP1-Mediated Regulation of HY5 Protein Accumulation in Light

COP1-mediated skotomorphogenic growth depends on the degradation of photomorphogenesis-promoting factors such as HY5, HYH, LAF1, HFR1, and BBX proteins. We tested if MYC3/MYC4 regulates HY5 protein accumulation through COP1. To address this, we grew Col-0, *cop1-4*, *myc3*, *myc4*, *myc3cop1-4, myc4cop1-4*, and *myc34cop1-4* genotypes in DD for 6 days and checked for HY5 protein levels using anti-HY5 antibody. Our data suggest that HY5 protein was elevated in the *cop1-4* mutant background in both dark and light conditions compared to Col-0 (Figure 7a–f). While in the *myc3cop1-4* and *myc4cop1-4* mutants, the levels of HY5 protein was comparable to *cop1-4*, it was further enhanced in the *myc34cop1-4* mutant compared to Col-0 (Figure 7a,b). When DD-grown seedlings were transferred to WL for 8h, HY5 protein accumulated more in the *myc34cop1-4* triple mutants than Col-0, while in *myc3cop1-4* and *myc4cop1-4* double mutants, its protein accumulation was comparable to *cop1-4* (Figure 7c,d). In the *myc3* and *myc4* single mutants, the HY5 protein level was largely comparable to Col-0 (Figure 7c,d). In WL-grown seedlings under SD, the HY5 protein was slightly enhanced in the *myc34cop1-4* than Col-0, but in the *myc3cop1-4* and *myc4cop1-4* mutants, HY5 protein levels was comparable to *cop1-4* (Figure 7e,f). The *myc3* and *myc4* mutants showed similar levels of HY5 protein accumulation as Col-0 (Figure 7e,f). These results suggest that MYC3 and MYC4, while individually, do not have any effect, but together likely have a weak influence on COP1 in controlling HY5 protein accumulation.

3.13 | MYC3 and MYC4 Are Targeted by COP1 for Degradation Thorough 26S Proteasomal Pathway

Our results suggest that MYC3 and MYC4 interfere with COP1-mediated hypocotyl and photo-pigment accumulation. We sought to examine if COP1 regulates MYC3 and MYC4 protein stability. To address this, we introgressed *35S:MYC3-GFP* and *35S:MYC4-GFP* transgenes into the *cop1-4* mutant background and identified homozygous *cop1-4 35S:MYC3-GFP* and *cop1-4 35S:MYC4-GFP* lines. Immunoblot analysis of MYC3 and MYC4 protein stability from 6-day-old DD-grown seedlings revealed that MYC3 protein was not detected as highly unstable (Figure 8a), while MYC4 protein was moderately stable (Figure 8a), as observed above. Interestingly, in the *cop1-4* mutant background, MYC3-GFP was stabilized (Figure 8a), suggesting that MYC3 is probably under the tight control of COP1. Similarly, MYC4-GFP protein stability was also elevated in the *cop1-4* mutant background compared to the *35S:MYC4-GFP* transgenic line (*35S:MYC4-GFP* transgenic line are in Col-0 background, hereafter referred to Col-0) (Figure 8a), suggesting that COP1 degrades MYC4 protein as well in the dark. Similar to DD, MYC3-GFP was stabilized in the *cop1-4* mutant background under WL (Figure 8b) and in different wavelengths of light (Figure 8c–e), suggesting that COP1 targets MYC3 degradation is probably both in dark and light conditions. On the other hand, unlike MYC3, the stability of MYC4-GFP protein in

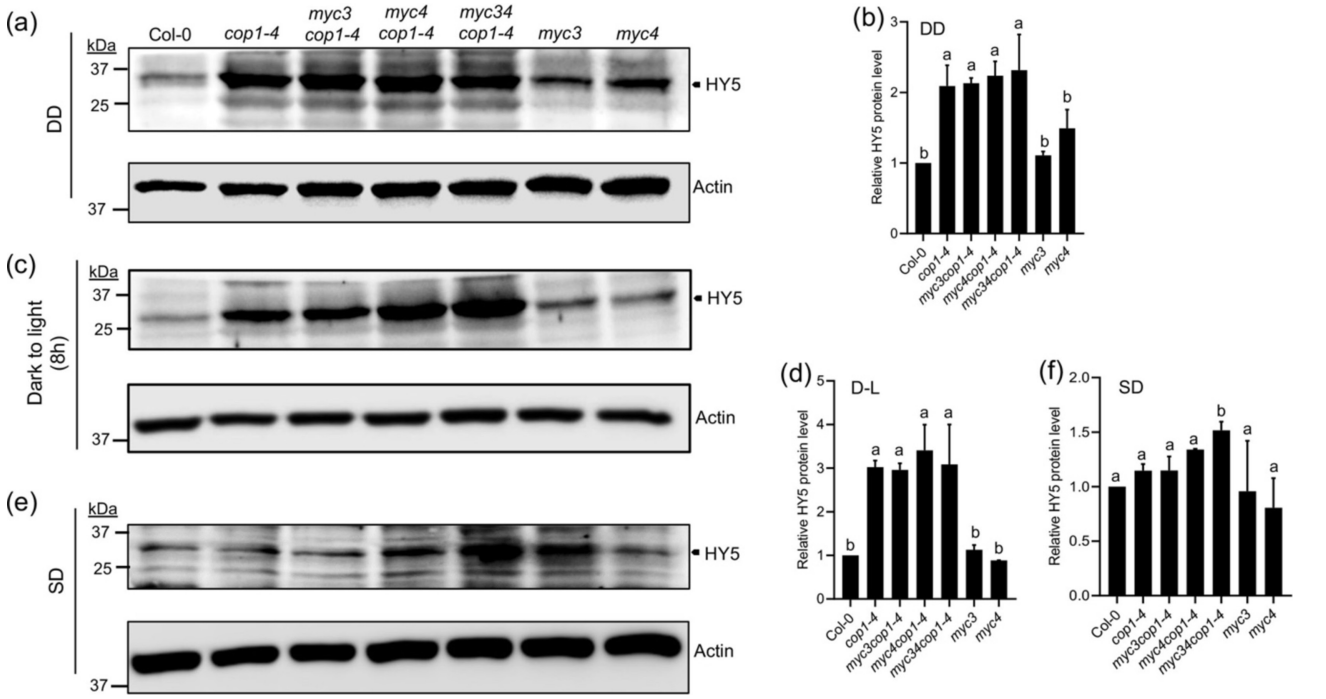

FIGURE 7 | MYC4 probably modulates COP1 in the degradation of HY5 and modulation of seedling photomorphogenesis. (a–f) Representative immunoblots and relative HY5 protein levels using native HY5 antibody in Col-0, *cop1-4, myc3cop1-4, myc4cop1-4, myc3myc4cop1-4, myc3*, and *myc4* mutants under constant dark (DD) (a and b), from constant dark to light treated for 8 h (c and d), and at ZT4 under SD (e and f). Actin was used as a control for all the blots and normalization. Relative protein levels from each immunoblot were calculated using ImageJ software. The immunoblots were repeated twice. Different letters above the bar chart indicate a significant difference (one-way ANOVA with Tukey's HSD test, $p < 0.05$).

the *cop1-4* mutant was comparable to Col-0 in WL and BL conditions (Figure 8b,c). However, in the RL and FRL conditions, MYC4-GFP protein levels was higher in the *cop1-4* mutant background than Col-0 (Figure 8d,e), suggesting that degradation of MYC4 protein by COP1 is wavelength-dependent.

Further, to know if COP1-mediated degradation of MYC3 and MYC4 is through the 26S proteasomal pathway, we grew *35S:MYC3-GFP*, *cop1-4 35S:MYC3-GFP*, *35S:MYC4-GFP* and *cop1-4 35S:MYC4-GFP* seedlings in DD for 5 days, and on the sixth day, they were treated with either DMSO (mock) or MG132 (50 μM) for 16 h, and total protein was extracted and carried out immunoblotting. Our data suggest that in the MG132-treated samples, the MYC3-GFP was stable, but not in the mock (Figure 8f), as seen above. Similarly, MYC4-GFP was more stable in the MG132-treated samples than the mock in the wild-type background (Figure 8g); however, in the *cop1-4* mutant background, the stability of MYC4-GFP was comparable between MG132-treated samples and mock (Figure 8g). In WL-grown seedlings under LD, MG132 treatment slightly stabilized MYC3-GFP in the wildtype background, while in the *cop1-4* mutants, its stability was comparable to the mock (Figure 8h). The MYC4-GFP protein stability was comparable to the mock in the wild-type background in WL-LD (Figure 8i). In the *cop1-4* mutant background, MYC4-GFP protein stability in the MG132 samples was slightly increased to the mock, suggesting that COP1 probably promotes degradation of MYC4 protein in the light as well. Together, these results confirm that COP1 targets MYC3 for degradation in the dark and all the wavelengths of light, including WL. However, COP1 degrades MYC4, specifically in the dark, RL, and FRL conditions, but not in WL and BL.

3.14 | COP1 Physically Interacts and Ubiquitinates MYC3 and MYC4 Before Degradation

To understand in more detail whether COP1-mediated degradation of MYC3 and MYC4 is through direct physical interaction, we performed an in vivo co-immunoprecipitation assay from *35S:MYC3-GFP* and *35S:MYC4-GFP* transgenic seedlings grown in DD for 5 days and treated with MG132 for 16 h. Our immunoblot data suggests that when COP1 was immunoprecipitated using an anti-COP1 antibody, we could detect MYC3-GFP (Figure 9a) and MYC4-GFP (Figure 9b) in the immunoprecipitated complex using an anti-GFP antibody. However, in the Col-0 that was used as a negative control, we could not detect MYC3-GFP (Figure 9a) or MYC4-GFP (Figure 9b) in the immunoprecipitated samples. These results suggested that COP1 physically interacts with MYC3 and MYC4. These physical interactions were further confirmed by a Biomolecular fluorescence complementation (BiFC) assay in the onion epidermal cells. When cYFP-COP1 was co-infiltrated with nYFP-MYC3 or nYFP-MYC4, strong YFP fluorescence was detected in the nucleus (color changed to green), as shown by the DAPI stain (Figure 9c). However, when cYFP/nYFP-MYC3, cYFP/nYFP-MYC4, cYFP-COP1/nYFP, and nYFP/cYFP empty vector combinations were co-infiltrated, no fluorescence was detected (Figure 9c), confirming that MYC3 and MYC4 physically associate with COP1.

Proteasomal degradation of substrates by COP1 requires ubiquitination of its target proteins (Osterlund et al. 2000; Holm et al. 2002; Seo et al. 2004; Kahle et al. 2020). As COP1 physically interacts with MYC3 and MYC4 and degrades them, we

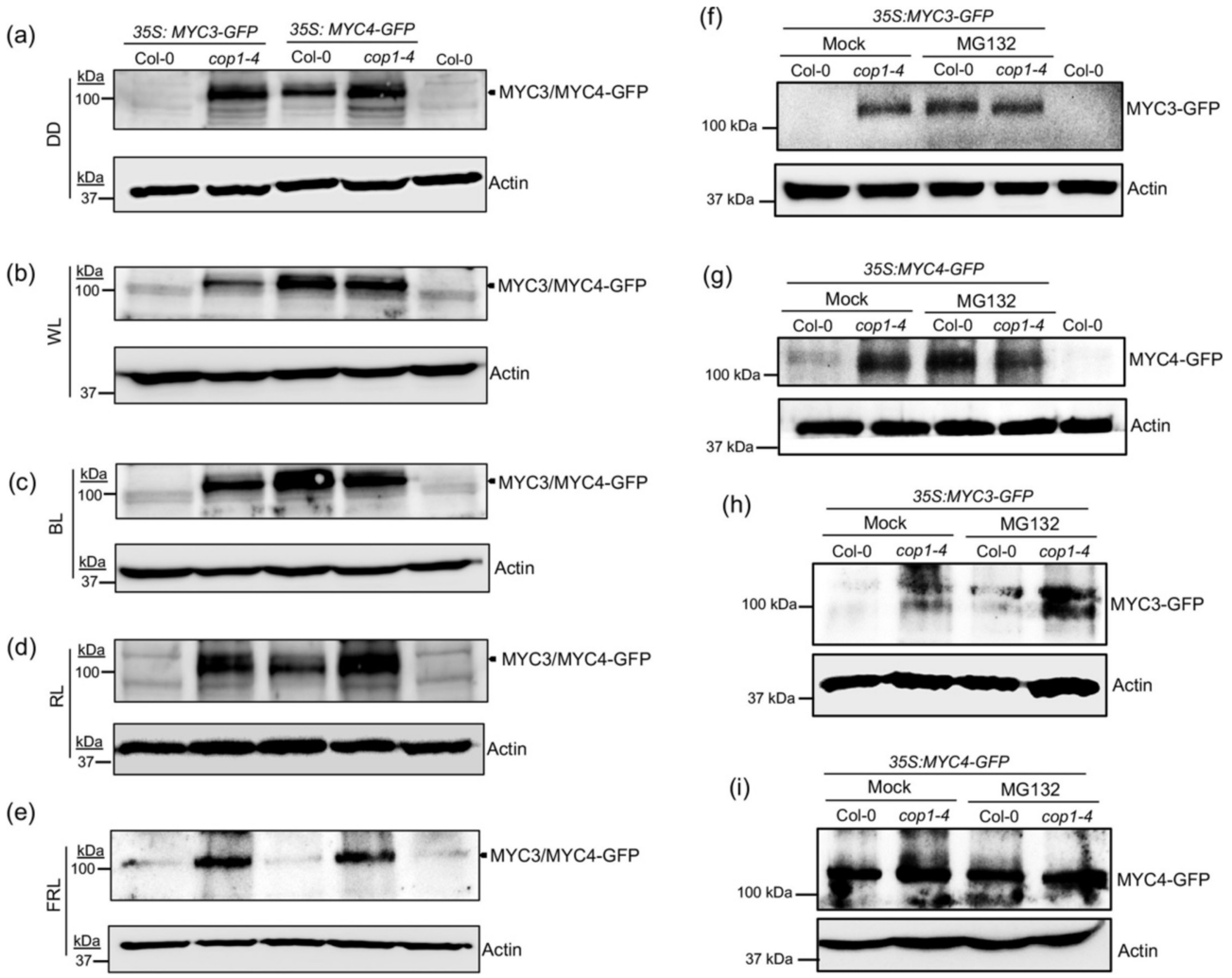

FIGURE 8 | COP1 targets MYC3 and MYC4 for proteasomal degradation. (a–e) MYC3 and MYC4 proteins are stabilized by 26S proteasome inhibitor (MG132). Immunoblot analysis showing MYC3/MYC4 protein stability in *35S:MYC3-GFP, cop1-4 35S:MYC3-GFP, 35S:MYC4-GFP*, and *cop1-4 35S:MYC4-GFP* seedlings grown under DD (a), and in WL (100 μmol m^{-2} s^{-1}) (b), BL (35 μmol m^{-2} s^{-1}) (c), RL (60 μmol m^{-2} s^{1}) (d), and FRL (0.5 μmol m^{-2} s^{1}) (e), under SD photoperiod (ZT4). (f and g) Immunoblot analysis of MYC3 (f) and MYC4 (g) protein stability in *35S:MYC3-GFP* and *cop1-4 35S:MYC3-GFP* seedlings grown in DD. MYC3-GFP/MYC4-GFP protein stability is elevated in MG132-treated seedlings in the wild-type background, similar to mock in the *cop1-4* background. (h and i) The MYC3 (h) and MYC4 (i) protein stability protein stability in *35S:MYC3-GFP, cop1-4 35S:MYC3-GFP, 35S:MYC4-GFP*, and *cop1-4 35S:MYC4-GFP* seedlings grown in WL LD, harvested at ZT4. In the presence of MG132, MYC3 protein gets stabilized, comparable to the DMSO-treated (mock) *cop1-4 35S:MYC3-GFP* seedlings. MYC4 protein stability was not altered in the MG132-treated samples compared to the mock, which is also similar in the *cop1-4* mutant background, suggesting COP1 does not control MYC4 protein stability in light. In (a)–(e), the total protein was extracted and subjected to immunoblot analysis using an anti-GFP antibody. Actin was used as a loading control.

were interested to know if COP1 ubiquitinates MYC3 and MYC4 before degradation. To check this, we used *35S:MYC3-GFP*, *cop1-4 35S:MYC3-GFP*, *35S:MYC4-GFP* and *cop1-4 35S:MYC4-GFP* transgenic lines grown in DD for 5 days and treatment with MG132 for 16 h, followed by protein extraction and immunoprecipitation with anti-GFP antibody. When we analyzed these immunoprecipitated samples using an anti-ubiquitin (αUbn) antibody, we could detect the ubiquitinated (Ubn) form of MYC3 and MYC4 proteins (Figure 9d,e), as both the proteins showed increased molecular weight (≥110 kDa) as compared to the non-ubiquitinated form (~110 kDa) (Figure 9d,e). Moreover, the stability of the ubiquitinated versions of MYC3-GFP and MYC4-GFP was reduced in the *cop1-4* mutant comparison to the wild-type background (Figure 9d,e). Analysis of immunoprecipitated complex using anti-GFP antibody showed the protein stability of MYC3-GFP and MYC4-GFP was comparable between Col-0 and the *cop1-4* mutant backgrounds (Figure 9d,e). These results confirm that COP1 ubiquitinates and degrades MYC3 and MYC4 in the dark to optimize seedling skotomorphogenic growth.

4 | Discussion

MYC transcription factors emerged as major regulators of growth and development in addition to their role in defense responses to herbivory and plant pathogens. Among MYCs, MYC2 is a dominant player regulating plant defense responses, while MYC3 and MYC4 act largely redundantly with

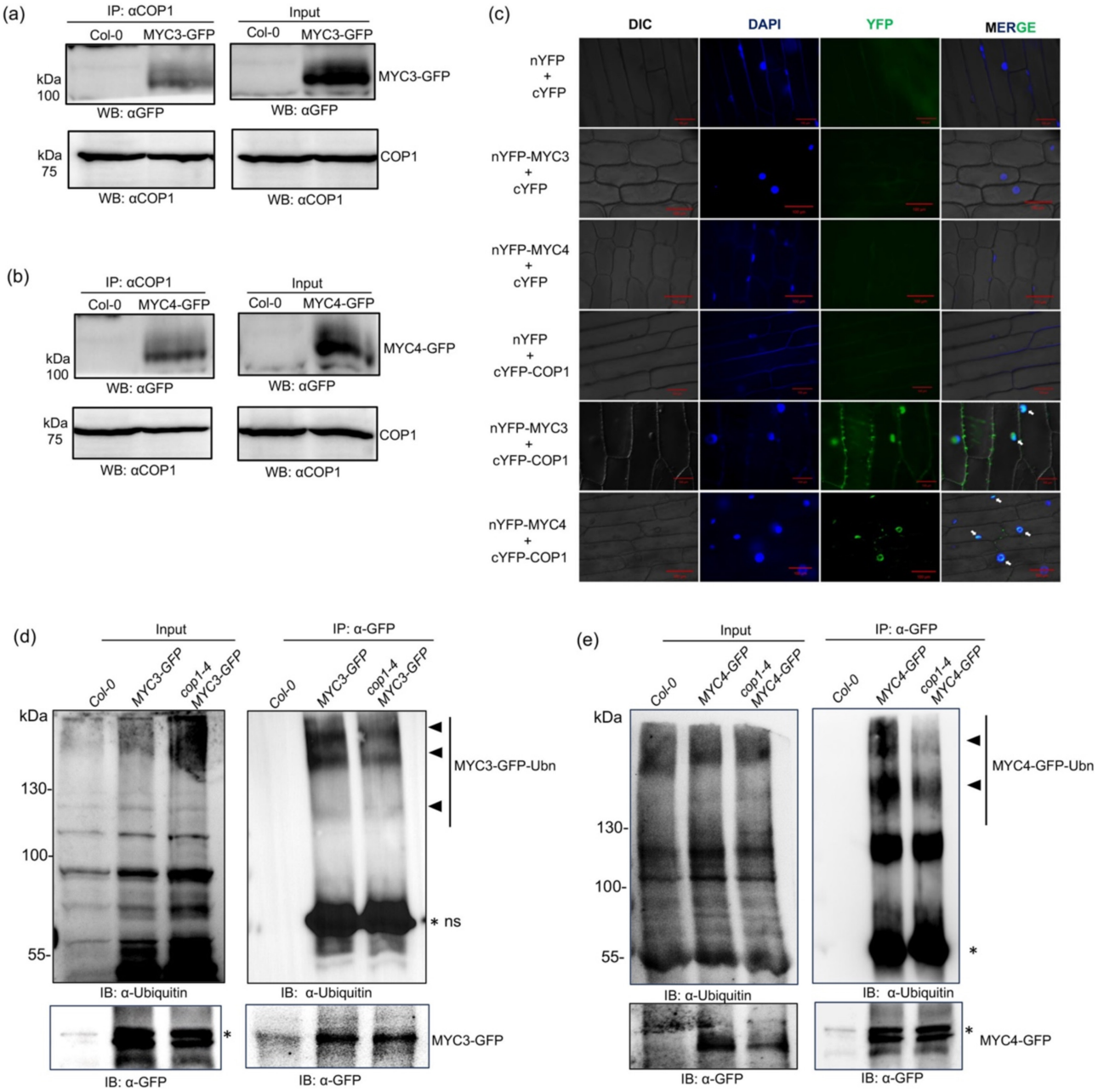

FIGURE 9 | COP1 ubiquitinates and degrades MYC3 and MYC4, probably through direct physical interaction. (a and b) The co-immunoprecipitation assays reveal that COP1 physically interacts with MYC3 (a) and MYC4 (b). For the MYC3 Co-IP experiment, 5-day-old seedlings of *35S:MYC3-GFP* grown in DD conditions were treated with the proteasomal inhibitor MG132 (50 μM) for 16 h, while for the MYC4 Co-IP assay, *35S:MYC4-GFP* seedlings were not treated with MG132. The issue was harvested, and protein was extracted. Total protein was used for immunoprecipitation using anti-COP1 antibody. The immunoprecipitated protein complex was analyzed for MG132 treated (50 μM) MYC3-GFP and MYC4-GFP using anti-GFP antibodies. (c) BiFC assay for physical interaction between MYC3/MYC4 and COP1. All the constructs containing nYFP and cYFP were co-transformed into onion epidermal cells. The positive interactions were observed in nYFP-MYC3/cYFP-COP1 and nYFP-MYC4/cYFP-COP1 but in the negative control combinations. The left panel image shows the bright field image (DIC), the middle panel shows the nucleus staining by DAPI, and the next panel shows the YFP channel produced by the reconstruction of YFP. The right panel image shows the merged image. The Arrows indicate the reconstituted YFP signal in the nuclei. The images were taken under 40X magnification. Scale bar = 100 μm.(d and e) In vivo ubiquitination assays show that COP1 ubiquitinates MYC3 (d) and MYC4 (e) in the dark, as the ubiquitinated MYC3 and MYC4 levels decreased in the *cop1-4* mutant. Five-day-old etiolated *35S:MYC3-GFP* and *35S:MYC4-GFP* transgenic seedlings were treated with 50 μM MG132 in liquid MS for 16 h, followed by immunoprecipitation with magnetic beads conjugated with anti-GFP antibody. Input and IP samples were detected using anti-ubiquitin (upper panel) and anti-GFP (lower panel) antibodies. The asterisks indicate non-specific bands.

MYC2 (Niu, Figueroa, and Browse 2011; Ortigosa et al. 2020). Specifically, the role of MYC2 in light-mediated seedling development has been well-established (Yadav et al. 2005; Gangappa, Prasad, and Chattopadhyay 2010; Gangappa et al. 2013b; Sethi et al. 2014; Chakraborty et al. 2019; Ortigosa et al. 2020; Srivastava et al. 2022). However, the role of MYC3

and MYC4 and their interaction with MYC2 in the seedling photomorphogenesis was unknown. This study demonstrates the coordinated interaction between MYC2/MYC3/MYC4 in regulating seedling photomorphogenic growth. Through genetic and molecular analyses, we have uncovered the multifaceted roles of MYC3 and MYC4 in modulating various aspects of light-mediated growth and development, shedding light on their interplay with key regulatory factors such as COP1 and HY5.

Our study unravels MYC4 as a negative regulator of seedling photomorphogenesis in a wavelength-independent manner. While MYC3 is found to have a minor role on its own, together with MYC4, it strongly enhances the photomorphogenic growth of hypocotyl as a double mutant of *myc3myc4* displayed significantly longer hypocotyls than the *myc3* and *myc4* (Figure 1). However, contrary to their role in hypocotyl growth, MYC3 and MYC4 together inhibit cotyledon photomorphogenic growth as the *myc3myc4* double mutant has bigger cotyledons than the *myc3* and *myc4* (Figure S3). The lack of cotyledon phenotype in the *myc4* mutant confirmed that MYC4 functions partially redundantly with MYC3 in inhibiting cotyledon expansion in response to light. These results suggested that MYC3 and MYC4 have independent and interdependent functions and display unequal redundancy in regulating seedling hypocotyl and cotyledon growth (Figure 1). Consistent with the hypocotyl growth phenotype, MYC transcription factors differentially regulate the anthocyanin and chlorophyll accumulation and the expression of light-inducible genes, as the anthocyanin, chlorophyll content, and gene expression levels in the triple mutants were very low compared to the single mutants, wherein it was either more or similar to wild-type (Figure 2). Similar to the role of MYC3 and MYC4 together in differentially regulating photomorphogenic growth in the hypocotyl and cotyledons, a bZIP transcription factor, GBF1/ZBF2, has also shown to inhibit photomorphogenesis in the hypocotyl but enhances in the cotyledons (Mallappa et al. 2006). Moreover, GBF1 genetically interacts with MYC2 and exhibits unequal genetic redundancy in regulating hypocotyl growth (Maurya et al. 2015).

Consistent with the *myc234* triple mutant phenotypes, such as long hypocotyl, reduced anthocyanin and chlorophyll accumulation, our results also revealed reduced HY5 protein accumulation in tested light conditions. HY5 is a key activator of genes involved in anthocyanin biosynthesis (Ang et al. 1998). The reduced expression of these genes in *myc234* triple mutants further supports our hypothesis that MYCs promote seedling photomorphogenesis by probably enhancing HY5 protein accumulation through the activation of its gene expression (Figures 2 and 5). Our results are also consistent with the earlier report that MYCs regulate *HY5* gene expression (Ortigosa et al. 2020). Therefore, the effect of MYCs on the regulation of *HY5* gene expression is possibly direct.

Our investigation into the genetic interaction between MYC3/MYC4 and HY5 revealed a nuanced regulatory mechanism governing hypocotyl growth. Our results demonstrate that MYC3 and MYC4 genetically interact with HY5 (Figure 4). The *myc3* and *myc4* mutations partially inhibit the *hy5* mutant phenotype; however, the ability to suppress *hy5* mutant hypocotyl length is slightly relieved in the presence of *myc3myc4* mutations. Notably, the *myc2* mutant was also shown to inhibit the *hy5* mutant growth phenotype (Srivastava, Dutta, and Chattopadhyay 2019), suggesting that MYCs individually act to inhibit HY5 function while together likely promoting HY5 function. The plausible mechanism by which the MYCs inhibit HY5 function is through physical interaction and inhibiting its transcriptional activity as MYC3/MYC4 (Figure 6) and MYC2 physically interact with HY5 (Srivastava, Dutta, and Chattopadhyay 2019). Together with earlier reports, our study underscores the dynamic and complex nature of regulatory networks controlling seedling development and emphasizes the role of MYC transcription factors in controlling HY5 for the precise regulation of photomorphogenesis.

Furthermore, our study uncovers that COP1 targets MYC3 and MYC4 for ubiquitination and subsequent proteasomal degradation, thereby modulating their abundance in response to light stimuli. COP1 exerts a stricter control on MYC3 under dark and light conditions, as MYC3-GFP is stable only in the *cop1-4* background or when the MYC3 seedlings were treated with the proteasomal inhibitor MG132 (Figure 8). Our data shows that the *myc3* mutant alone does not display any visible changes in the hypocotyl length, while in the *myc2* and *myc4* background, it modulates their phenotype. These results imply that MYC3 is likely playing a crucial role in regulating the functions of MYC2 and MYC4, and therefore, COP1 plays a role in this modulation by maintaining very low MYC3 protein levels. While MYC4 is also targeted by COP1 for ubiquitination and degradation, unlike MYC3, MYC4 protein remains present in dark and light conditions, albeit at a lower level (Figure 8). Consistent with increased MYC3 and MYC4 protein stability in the dark upon MG132 treatment, the ubiquitinated form of MYC3-GFP and MYC4-GFP was visibly reduced in the *cop1-4* mutant compared to wild-type seedlings, suggesting that the absence of COP1 results reduced ubiquitination and enhanced MYC3/MYC4 protein stability likely due to lack of physical interactions between MYC3 and MYC4 with COP1 (Figure 9). Similar to MYC3 and MYC4, COP1 also targets MYC2 for degradation under constant dark and diurnal light/dark conditions (Chico et al. 2014), suggesting that COP1 plays a critical role in maintaining optimal concentrations of MYC transcription factors in dark and light conditions, whose effect further impinges on HY5 in fine-tuning seedling photomorphogenic growth (Figure 10). Our findings are consistent with previous reports highlighting the pivotal role of COP1 in orchestrating light-mediated developmental processes by regulating the stability of key transcription factors, including MYC proteins (Osterlund, Wei, and Deng 2000; Holm et al. 2002; Saijo et al. 2003; Seo et al. 2004). In summary, our study provides a mechanistic insight into the complex interplay among MYC transcription factors with HY5 and COP1 to regulate seedling photomorphogenesis in response to varying light conditions.

Limitations of the Study

The major limitation of this study is that it was unable to detect MYC3 protein in the MYC3-GFP transgenic line, even though it overexpresses the *MYC3* transcript. It would have been interesting to understand how this connects to the *myc3* mutant phenotypes. Second, an additional triple mutant of *myc234* generated from a different *myc2* mutant allele other than *jin1-2* would have clarified whether some of the phenotypes we have observed in

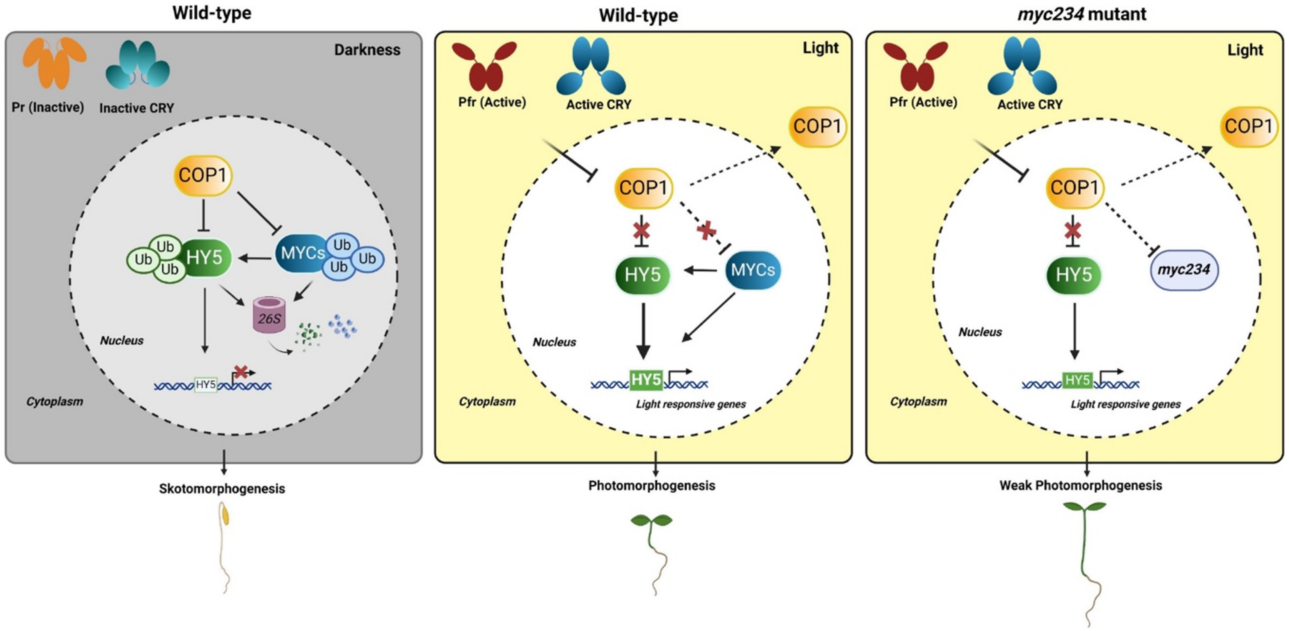

FIGURE 10 | Working model of MYC transcription factors in the regulation of seedling photomorphogenesis. In the dark, COP1 targets HY5 for degradation to promote skotomorphogenesis. At the same time, COP1 also degrades MYCs for optimal skotomorphogenic growth. In the light, photoreceptor-mediated inhibition of COP1 and partial depletion of COP1 from the nucleus due to cytosol result in enhanced HY5 accumulation. Also, enhanced accumulation of MYCs leads to increased HY5 activity, which leads to optimal photomorphogenic growth. It is also likely that MYCs together promote photomorphogenesis independent of HY5. The absence of all the MYCs (*myc234* triple mutant) reduces HY5 activity, due to reduced *HY5* transcript accumulation, resulting in weak photomorphogenic growth. In summary, MYC2/3/4 together promotes photomorphogenesis by enhancing HY5 function, while individually, they act as negative regulators of photomorphogenesis.

the *myc234* are due to the *cop1-21* mutation.It will be interesting to address in the future.

Author Contributions

S.N.G. conceptualized and supervised the study. V.G. planned and conducted most experiments, collected results, analyzed the data, and prepared figures. S.D. performed gene expression analysis. S.N.G. wrote the manuscript with the help of V.G and S.D. All the authors have read and approved the final version.

Acknowledgments

We thank all the members of the Gangappa laboratory for the helpful discussions. We also thank Dr. Channakeshavaiah C. for the BIFC binary vectors, Prof. Shubho Chaudhuri for the GV3101 agrobacterium strain, and Prof. Roberto Solano for the *jin1-2*, *35S:MYC3-GFP*, and *35S:MYC4-GFP* transgenic seeds. V.G. and S.D. acknowledge the University Grants Commission (UGC, Govt of India) and IISER Kolkata (Ministry of Education) for their doctoral fellowship. We also thank Prof. Sumana Annagiri (IISER Kolkata) for the microscopy and the BioRender software for helping us draw our model. This work was supported by grants from the Department of Biotechnology (Ramalingaswami Re-entry Fellowship grant, BT/RLF/Re-entry/28/2017), Science and Engineering Research Board (start-up research grant, SRG/2019/000446) from the Govt. of India, and Intramural grant from IISER Kolkata (Ministry of Education, Govt. of India) to S.N.G.

Conflicts of Interest

The authors declare no conflicts of interest.

Data Availability Statement

All the data presented in this study can be found in the main manuscript and the supporting information.

References

Abbas, N., J. P. Maurya, D. Senapati, S. N. Gangappa, and S. Chattopadhyay. 2014. "Arabidopsis CAM7 and HY5 Physically Interact and Directly Bind to the HY5 Promoter to Regulate Its Expression and Thereby Promote Photomorphogenesis." *Plant Cell* 26: 1036–1052.

Ang, L. H., S. Chattopadhyay, N. Wei, et al. 1998. "Molecular Interaction Between COP1 and HY5 Defines a Regulatory Switch for Light Control of Arabidopsis Development." *Molecular Cell* 1: 213–222.

Ang, L. H., and X. W. Deng. 1994. "Regulatory Hierarchy of Photomorphogenic Loci: Allele-Specific and Light-Dependent Interaction Between the HY5 and COP1 Loci." *Plant Cell* 6: 613–628.

Binkert, M., L. Kozma-Bognar, K. Terecskei, L. De Veylder, F. Nagy, and R. Ulm. 2014a. "UV-B-Responsive Association of the Arabidopsis bZIP Transcription Factor ELONGATED HYPOCOTYL5 With Target Genes, Including Its own Promoter." *Plant Cell* 26: 4200–4213.

Binkert, M., L. Kozma-Bognár, K. Terecskei, L. De Veylder, F. Nagy, and R. Ulm. 2014b. "UV-B-Responsive Association of the Arabidopsis bZIP Transcription Factor ELONGATED HYPOCOTYL5 With Target Genes, Including Its own Promoter." *Plant Cell* 26: 4200–4213.

Blanco-Touriñán, N., M. Legris, E. G. Minguet, et al. 2020. "COP1 Destabilizes DELLA Proteins in Arabidopsis." *Proceedings of the National Academy of Sciences of the United States of America* 117: 13792–13799.

Briggs, G. C., K. S. Osmont, C. Shindo, R. Sibout, and C. S. Hardtke. 2006. "Unequal Genetic Redundancies in Arabidopsis—A Neglected Phenomenon?" *Trends in Plant Science* 11: 492–498.

Burko, Y., A. Seluzicki, M. Zander, U. V. Pedmale, J. R. Ecker, and J. Chory. 2020. "Chimeric Activators and Repressors Define HY5 Activity and Reveal a Light-Regulated Feedback Mechanism." *Plant Cell* 32: 967–983.

Catalá, R., J. Medina, and J. Salinas. 2011. "Integration of Low Temperature and Light Signaling During Cold Acclimation Response in Arabidopsis." *Proceedings of the National Academy of Sciences of the United States of America* 108: 16475–16480.

Chakraborty, M., S. N. Gangappa, J. P. Maurya, et al. 2019. "Functional Interrelation of MYC2 and HY5 Plays an Important Role in Arabidopsis Seedling Development." *Plant Journal* 99: 1080–1097.

Chattopadhyay, S., L. H. Ang, P. Puente, X. W. Deng, and N. Wei. 1998. "Arabidopsis bZIP Protein HY5 Directly Interacts With Light-Responsive Promoters in Mediating Light Control of Gene Expression." *Plant Cell* 10: 673–683.

Cheng, M. C., P. K. Kathare, I. Paik, and E. Huq. 2021. "Phytochrome Signaling Networks." *Annual Review of Plant Biology* 72: 217–244.

Chico, J. M., G. Fernández-Barbero, A. Chini, P. Fernández-Calvo, M. Díez-Díaz, and R. Solano. 2014. "Repression of Jasmonate-Dependent Defenses by Shade Involves Differential Regulation of Protein Stability of MYC Transcription Factors and Their JAZ Repressors in Arabidopsis." *Plant Cell* 26: 1967–1980.

Datta, S., H. Johansson, C. Hettiarachchi, et al. 2008. "LZF1/SALT TOLERANCE HOMOLOG3, an Arabidopsis B-Box Protein Involved in Light-Dependent Development and Gene Expression, Undergoes COP1-Mediated Ubiquitination." *Plant Cell* 20: 2324–2338.

Deng, X. W., T. Caspar, and P. H. Quail. 1991. "cop1: A Regulatory Locus Involved in Light-Controlled Development and Gene Expression in Arabidopsis." *Genes & Development* 5: 1172–1182.

Dohmann, E. M., C. Kuhnle, and C. Schwechheimer. 2005. "Loss of the CONSTITUTIVE PHOTOMORPHOGENIC9 Signalosome Subunit 5 Is Sufficient to Cause the cop/det/fus Mutant Phenotype in Arabidopsis." *Plant Cell* 17: 1967–1978.

Dombrecht, B., G. P. Xue, S. J. Sprague, et al. 2007. "MYC2 Differentially Modulates Diverse Jasmonate-Dependent Functions in Arabidopsis." *Plant Cell* 19: 2225–2245.

Fernandez-Calvo, P., A. Chini, G. Fernandez-Barbero, et al. 2011. "The Arabidopsis bHLH Transcription Factors MYC3 and MYC4 Are Targets of JAZ Repressors and act Additively With MYC2 in the Activation of Jasmonate Responses." *Plant Cell* 23: 701–715.

Gangappa, S. N., and J. F. Botto. 2016. "The Multifaceted Roles of HY5 in Plant Growth and Development." *Molecular Plant* 9: 1353–1365.

Gangappa, S. N., C. D. Crocco, H. Johansson, et al. 2013a. "The Arabidopsis B-BOX Protein BBX25 Interacts With HY5, Negatively Regulating BBX22 Expression to Suppress Seedling Photomorphogenesis." *Plant Cell* 25: 1243–1257.

Gangappa, S. N., V. B. Prasad, and S. Chattopadhyay. 2010. "Functional Interconnection of MYC2 and SPA1 in the Photomorphogenic Seedling Development of Arabidopsis." *Plant Physiology* 154: 1210–1219.

Gangappa, S. N., A. K. Srivastava, J. P. Maurya, H. Ram, and S. Chattopadhyay. 2013b. "Z-Box Binding Transcription Factors (ZBFs): A new Class of Transcription Factors in Arabidopsis Seedling Development." *Molecular Plant* 6: 1758–1768.

Gao, C., S. Qi, K. Liu, et al. 2016. "MYC2, MYC3, and MYC4 Function Redundantly in Seed Storage Protein Accumulation in Arabidopsis." *Plant Physiology and Biochemistry* 108: 63–70.

Hayami, N., Y. Sakai, M. Kimura, et al. 2015. "The Responses of Arabidopsis Early Light-Induced Protein2 to Ultraviolet B, High Light, and Cold Stress Are Regulated by a Transcriptional Regulatory Unit Composed of Two Elements." *Plant Physiology* 169: 840–855.

Holm, M., L. G. Ma, L. J. Qu, and X. W. Deng. 2002. "Two Interacting bZIP Proteins Are Direct Targets of COP1-Mediated Control of Light-Dependent Gene Expression in Arabidopsis." *Genes & Development* 16: 1247–1259.

Huq, E., C. Lin, and P. H. Quail. 2024. "Light Signaling in Plants - A Selective History." *Plant Physiology* 195: 213–231.

Jang, I. C., J. Y. Yang, H. S. Seo, and N. H. Chua. 2005. "HFR1 Is Targeted by COP1 E3 Ligase for Post-Translational Proteolysis During Phytochrome a Signaling." *Genes & Development* 19: 593–602.

Jiao, Y., O. S. Lau, and X. W. Deng. 2007. "Light-Regulated Transcriptional Networks in Higher Plants." *Nature Reviews. Genetics* 8: 217–230.

Job, N., and S. Datta. 2021. "PIF3/HY5 Module Regulates BBX11 to Suppress Protochlorophyllide Levels in Dark and Promote Photomorphogenesis in Light." *New Phytologist* 230: 190–204.

Kahle, N., D. J. Sheerin, P. Fischbach, et al. 2020. "COLD REGULATED 27 and 28 Are Targets of CONSTITUTIVELY PHOTOMORPHOGENIC 1 and Negatively Affect Phytochrome B Signalling." *Plant Journal* 104: 1038–1053.

Koornneef, M., E. Rolff, and C. J. P. Spruit. 1980. "Genetic Control of Light-Inhibited Hypocotyl Elongation in Arabidopsis Thaliana (L.) Heynh." *Zeitschrift für Pflanzenphysiologie* 100: 147–160.

Krahmer, J., and C. Fankhauser. 2023. "Environmental Control of Hypocotyl Elongation." *Annual Review of Plant Biology* 75: 489–519.

Lau, O. S., and X. W. Deng. 2012. "The Photomorphogenic Repressors COP1 and DET1: 20 Years Later." *Trends in Plant Science* 17: 584–593.

Laubinger, S., K. Fittinghoff, and U. Hoecker. 2004. "The SPA Quartet: A Family of WD-Repeat Proteins With a Central Role in Suppression of Photomorphogenesis in Arabidopsis." *Plant Cell* 16: 2293–2306.

Lee, J., K. He, V. Stolc, et al. 2007. "Analysis of Transcription Factor HY5 Genomic Binding Sites Revealed Its Hierarchical Role in Light Regulation of Development." *Plant Cell* 19: 731–749.

Li, C., K. Nozue, and J. N. Maloof. 2020. "MYCs and PIFs act Independently in Arabidopsis." *Growth Regulation. G3 (Bethesda)* 10: 1797–1807.

Li, C., L. Qi, S. Zhang, et al. 2022. "Mutual Upregulation of HY5 and TZP in Mediating Phytochrome a Signaling." *Plant Cell* 34: 633–654.

Lorenzo, O., J. M. Chico, J. J. Sánchez-Serrano, and R. Solano. 2004. "JASMONATE-INSENSITIVE1 Encodes a MYC Transcription Factor Essential to Discriminate Between Different Jasmonate-Regulated Defense Responses in Arabidopsis." *Plant Cell* 16: 1938–1950.

Luo, F., Q. Zhang, H. Xin, et al. 2022. "A Phytochrome B-PIF4-MYC2/MYC4 Module Inhibits Secondary Cell Wall Thickening in Response to Shaded Light." *Plant Communications* 3: 100416.

Mallappa, C., V. Yadav, P. Negi, and S. Chattopadhyay. 2006. "A Basic Leucine Zipper Transcription Factor, G-Box-Binding Factor 1, Regulates Blue Light-Mediated Photomorphogenic Growth in Arabidopsis*." *Journal of Biological Chemistry* 281: 22190–22199.

Maurya, J. P., V. Sethi, S. N. Gangappa, N. Gupta, and S. Chattopadhyay. 2015. "Interaction of MYC2 and GBF1 Results in Functional Antagonism in Blue Light-Mediated Arabidopsis Seedling Development." *Plant Journal* 83: 439–450.

McNellis, T. W., A. G. von Arnim, T. Araki, Y. Komeda, S. Miséra, and X. W. Deng. 1994. "Genetic and Molecular Analysis of an Allelic Series of cop1 Mutants Suggests Functional Roles for the Multiple Protein Domains." *Plant Cell* 6: 487–500.

Nagatani, A., J. W. Reed, and J. Chory. 1993. "Isolation and Initial Characterization of Arabidopsis Mutants That Are Deficient in Phytochrome a." *Plant Physiology* 102: 269–277.

Neff, M. M., C. Fankhauser, and J. Chory. 2000. "Light: An Indicator of Time and Place." *Genes & Development* 14: 257–271.

Niu, Y., P. Figueroa, and J. Browse. 2011. "Characterization of JAZ-Interacting bHLH Transcription Factors That Regulate Jasmonate Responses in Arabidopsis." *Journal of Experimental Botany* 62: 2143–2154.

Ojha, M., D. Verma, N. Chakraborty, et al. 2023. "MKKK20 Works as an Upstream Triple-Kinase of MKK3-MPK6-MYC2 Module in Arabidopsis Seedling Development." *iScience* 26: 106049.

Ortigosa, A., S. Fonseca, J. M. Franco-Zorrilla, et al. 2020. "The JA-Pathway MYC Transcription Factors Regulate Photomorphogenic Responses by Targeting HY5 Gene Expression." *Plant Journal* 102: 138–152.

Osterlund, M. T., C. S. Hardtke, N. Wei, and X. W. Deng. 2000. "Targeted Destabilization of HY5 During Light-Regulated Development of Arabidopsis." *Nature* 405: 462–466.

Osterlund, M. T., N. Wei, and X. W. Deng. 2000. "The Roles of Photoreceptor Systems and the COP1-Targeted Destabilization of HY5 in Light Control of Arabidopsis Seedling Development." *Plant Physiology* 124: 1520–1524.

Oyama, T., Y. Shimura, and K. Okada. 1997. "The Arabidopsis HY5 Gene Encodes a bZIP Protein That Regulates Stimulus-Induced Development of Root and Hypocotyl." *Genes & Development* 11: 2983–2995.

Ram, H., and S. Chattopadhyay. 2013. "Molecular Interaction of bZIP Domains of GBF1, HY5 and HYH in Arabidopsis Seedling Development." *Plant Signaling & Behavior* 8: e22703.

Saijo, Y., J. A. Sullivan, H. Wang, et al. 2003. "The COP1-SPA1 Interaction Defines a Critical Step in Phytochrome A-Mediated Regulation of HY5 Activity." *Genes & Development* 17: 2642–2647.

Seo, H. S., E. Watanabe, S. Tokutomi, A. Nagatani, and N. H. Chua. 2004. "Photoreceptor Ubiquitination by COP1 E3 Ligase Desensitizes Phytochrome a Signaling." *Genes & Development* 18: 617–622.

Seo, H. S., J. Y. Yang, M. Ishikawa, C. Bolle, M. L. Ballesteros, and N. H. Chua. 2003. "LAF1 Ubiquitination by COP1 Controls Photomorphogenesis and Is Stimulated by SPA1." *Nature* 423: 995–999.

Sethi, V., B. Raghuram, A. K. Sinha, and S. Chattopadhyay. 2014. "A Mitogen-Activated Protein Kinase Cascade Module, MKK3-MPK6 and MYC2, Is Involved in Blue Light-Mediated Seedling Development in Arabidopsis." *Plant Cell* 26: 3343–3357.

Sibout, R., P. Sukumar, C. Hettiarachchi, M. Holm, G. K. Muday, and C. S. Hardtke. 2006. "Opposite Root Growth Phenotypes of hy5 Versus hy5 hyh Mutants Correlate With Increased Constitutive Auxin Signaling." *PLoS Genetics* 2: e202.

Song, Z., T. Yan, J. Liu, et al. 2020. "BBX28/BBX29, HY5 and BBX30/31 Form a Feedback Loop to Fine-Tune Photomorphogenic Development." *Plant Journal* 104: 377–390.

Srivastava, A. K., S. Dutta, and S. Chattopadhyay. 2019. "MYC2 Regulates ARR16, a Component of Cytokinin Signaling Pathways, in Arabidopsis Seedling Development." *Plant Direct* 3: e00177.

Srivastava, M., A. K. Srivastava, D. Roy, et al. 2022. "The Conjugation of SUMO to the Transcription Factor MYC2 Functions in Blue Light-Mediated Seedling Development in Arabidopsis." *Plant Cell* 34: 2892–2906.

Van Moerkercke, A., O. Duncan, M. Zander, et al. 2019. "A MYC2/MYC3/MYC4-Dependent Transcription Factor Network Regulates Water Spray-Responsive Gene Expression and Jasmonate Levels." *Proceedings of the National Academy of Sciences of the United States of America* 116: 23345–23356.

Wang, D. D., P. Li, Q. Y. Chen, et al. 2021. "Differential Contributions of MYCs to Insect Defense Reveals Flavonoids Alleviating Growth Inhibition Caused by Wounding in Arabidopsis." *Frontiers in Plant Science* 12: 700555.

Wei, N., and X. W. Deng. 1999. "Making Sense of the COP9 Signalosome. A Regulatory Protein Complex Conserved From Arabidopsis to Human." *Trends in Genetics* 15: 98–103.

Whitelam, G. C., E. Johnson, J. Peng, et al. 1993. "Phytochrome a Null Mutants of Arabidopsis Display a Wild-Type Phenotype in White Light." *Plant Cell* 5: 757–768.

Xu, D., Y. Jiang, J. Li, F. Lin, M. Holm, and X. W. Deng. 2016. "BBX21, an Arabidopsis B-Box Protein, Directly Activates HY5 and Is Targeted by COP1 for 26S Proteasome-Mediated Degradation." *Proceedings of the National Academy of Sciences of the United States of America* 113: 7655–7660.

Yadav, V., C. Mallappa, S. N. Gangappa, S. Bhatia, and S. Chattopadhyay. 2005. "A Basic helix-Loop-helix Transcription Factor in Arabidopsis, MYC2, Acts as a Repressor of Blue Light-Mediated Photomorphogenic Growth." *Plant Cell* 17: 1953–1966.

Yang, J., R. Lin, J. Sullivan, et al. 2005. "Light Regulates COP1-Mediated Degradation of HFR1, a Transcription Factor Essential for Light Signaling in Arabidopsis." *Plant Cell* 17: 804–821.

Yu, D., X. Dong, K. Zou, et al. 2023. "A Hidden Mutation in the Seventh WD40-Repeat of COP1 Determines the Early Flowering Trait in a set of Arabidopsis myc Mutants." *Plant Cell* 35: 345–350.

Zhang, C., Y. Lei, C. Lu, L. Wang, and J. Wu. 2020. "MYC2, MYC3, and MYC4 Function Additively in Wounding-Induced Jasmonic Acid Biosynthesis and Catabolism." *Journal of Integrative Plant Biology* 62: 1159–1175.

Zhang, Q., Z. Xie, R. Zhang, et al. 2018. "Blue Light Regulates Secondary Cell Wall Thickening via MYC2/MYC4 Activation of the NST1-Directed Transcriptional Network in Arabidopsis." *Plant Cell* 30: 2512–2528.

Zhang, X., Z. Zhu, F. An, et al. 2014. "Jasmonate-Activated MYC2 Represses ETHYLENE INSENSITIVE3 Activity to Antagonize Ethylene-Promoted Apical Hook Formation in Arabidopsis." *Plant Cell* 26: 1105–1117.

Zheng, Y., X. Cui, L. Su, et al. 2017. "Jasmonate Inhibits COP1 Activity to Suppress Hypocotyl Elongation and Promote cotyledon Opening in Etiolated Arabidopsis Seedlings." *Plant Journal* 90: 1144–1155.

Supporting Information

Additional supporting information can be found online in the Supporting Information section.